



HAL
open science

Source-sink relationships during grain filling in wheat in response to various temperature, water deficit and nitrogen deficit regimes

Liang Fang, Paul C Struik, Christine Grousse, Xinyou Yin, Pierre Martre

► To cite this version:

Liang Fang, Paul C Struik, Christine Grousse, Xinyou Yin, Pierre Martre. Source-sink relationships during grain filling in wheat in response to various temperature, water deficit and nitrogen deficit regimes. *Journal of Experimental Botany*, 2024, 75 (20), pp.6563-6578. <10.1093/jxb/erae310>. <hal-04659404>

HAL Id: hal-04659404

<https://hal.inrae.fr/hal-04659404v1>

Submitted on 23 Jul 2024

HAL is a multi-disciplinary open access archive for the deposit and dissemination of scientific research documents, whether they are published or not. The documents may come from teaching and research institutions in France or abroad, or from public or private research centers.

L'archive ouverte pluridisciplinaire HAL, est destinée au dépôt et à la diffusion de documents scientifiques de niveau recherche, publiés ou non, émanant des établissements d'enseignement et de recherche français ou étrangers, des laboratoires publics ou privés.



Distributed under a Creative Commons CC BY-NC 4.0 - Attribution - Non-commercial use - International License

Source-sink relationships during grain filling in wheat in response to various temperature, water deficit and nitrogen deficit regimes

Liang Fang¹, Paul C. Struik¹, Christine Girousse², Xinyou Yin^{1*}, Pierre Martre^{3*}

¹ Centre for Crop Systems Analysis, Wageningen University & Research, Wageningen, The Netherlands

² GDEC, INRAE, Clermont Auvergne University, Clermont-Ferrand, France

³ LEPSE, Univ Montpellier, INRAE, Institut Agro Montpellier, Montpellier, France

*Author for correspondence:

Dr. Xinyou Yin, Centre for Crop Systems Analysis, Department of Plant Sciences, Wageningen University & Research, P.O. Box 430, 6700 AK Wageningen, The Netherlands

Email: xinyou.yin@wur.nl

Dr. Pierre Martre, LEPSE, Univ Montpellier, INRAE, Institut Agro Montpellier, Montpellier, France

Email: pierre.martre@inrae.fr

ORCID IDs

Liang Fang: <https://orcid.org/0000-0002-0989-0092>

Paul C. Struik: <https://orcid.org/0000-0003-2196-547X>

Christine Girousse: <https://orcid.org/0000-0002-8914-2878>

Xinyou Yin: <https://orcid.org/0000-0001-8273-8022>

Pierre Martre: <https://orcid.org/0000-0002-7419-6558>

© The Author(s) 2024. Published by Oxford University Press on behalf of the Society for Experimental Biology.

This is an Open Access article distributed under the terms of the Creative Commons Attribution-NonCommercial License (<https://creativecommons.org/licenses/by-nc/4.0/>), which permits non-commercial re-use, distribution, and reproduction in any medium, provided the original work is properly cited. For commercial re-use, please contact reprints@oup.com for reprints and translation rights for reprints. All other permissions can be obtained through our RightsLink service via the Permissions link on the article page on our site—for further information please contact journals.permissions@oup.com.

Highlight

Quantitative model-fitting analysis of data from 13-years' semi-field experiments identified increased contributions of remobilized pre-anthesis carbon and nitrogen to grain growth of wheat under stress conditions.

Accepted Manuscript

Abstract

Grain filling is a critical process for improving crop production under adverse conditions caused by climate change. Here, using a quantitative method, we quantified post-anthesis source-sink relationships of a large data set to assess the contribution of remobilized pre-anthesis assimilates to grain growth for both biomass and nitrogen. The data set came from 13 years' semi-controlled field experimentation, in which six bread wheat genotypes were grown at plot scale under contrasting temperature, water, and nitrogen regimes. On average, grain biomass was ~10% higher than post-anthesis aboveground biomass accumulation across regimes and genotypes. Overall, the estimated relative contribution (%) of remobilized assimilates to grain biomass became increasingly significant with increasing stress intensity, ranging from virtually nil to 100%. This percentage was altered more by water and nitrogen regimes than by temperature, indicating the greater impact of water or nitrogen regimes relative to high temperatures under our experimental conditions. Relationships between grain nitrogen demand and post-anthesis nitrogen uptake were generally insensitive to environmental conditions, as there was always significant remobilization of nitrogen from vegetative organs, which helped to stabilize the amount of grain nitrogen. Moreover, variations in the relative contribution of remobilized assimilates with environmental variables were genotype-dependent. Our analysis provides an overall picture of post-anthesis source-sink relationships and pre-anthesis assimilate contributions to grain filling across (non-)environmental factors, and highlights that designing wheat adaption to climate change should account for complex multi-factor interactions.

Keywords

Carbon, drought stress, extreme weather events, global warming, heat shock, nitrogen, remobilization, sink-source relationship, temperature, wheat.

1 Introduction

High temperatures and soil water deficit are two most pervasive stresses for crop production. Besides average overall warming and increases in drought intensity associated with ongoing climate change, extreme heat waves and severe-drought spells occur in a higher frequency. These climate-change events are threatening global food production and lead to uncertainty in global food supply in the future (Asseng et al., 2019; Yin & Struik, 2017; Zhao et al., 2017).

Yield of the grains harvested from cereal crops is co-determined by source (available net photosynthetic assimilates) and sink (the capacity of grains to utilize available assimilates) activities. There are dynamic feedback and feedforward interactions between source and sink, i.e., the sink strength can influence source activity and *vice versa* (Martre et al., 2003; Schapendonk et al., 2007; Dingkuhn et al. 2020; Reynolds et al., 2022). Yet, source and sink respond differently to environmental variables (Yin et al., 2009; Asseng et al., 2017; Shi et al., 2017; Shao et al., 2021; Reynolds et al., 2022). Therefore, quantifying how source and sink respond to different environmental variables and their interactions is essential when assessing the impacts of climate change and designing agricultural adaptation strategies.

Carbon assimilates for grain growth may come mainly from post-anthesis photosynthesis. High temperatures, including long-term elevated growth temperatures (HT) and short-term extremely high temperatures (heat shocks, HS) accelerate crop phenology and leaf senescence, thereby reducing the durations of photo-assimilates accumulation and grain filling (Barnabás et al., 2008; Asseng et al., 2015, 2019). However, a higher grain filling rate may partly compensate for the shorter grain filling duration under moderately high temperatures (Yin et al., 2009), but this may require an increased remobilization of (pre-anthesis) assimilate reserves stored in vegetative organs. Nevertheless, high temperatures that are within the supra-optimal range will suppress photosynthesis (Fang et al., 2023). Water deficit (WD) suppresses photosynthesis mainly by reducing CO₂ diffusional conductance and limiting photosynthetic biochemical processes (Wei et al., 2020; Fang et al., 2023), but also via an accelerated whole-plant senescence (Evans, 1993). Yet, the effects of WD on grain filling rate were inconsistent in previous studies where decreased (Yang et al., 2006), unaffected (Nicolas et al., 1984) and increased (Yang & Zhang, 2006) grain filling rates under WD conditions were reported. Further, the impacts of high temperatures and water stress could be variable, depending on the timing of

the stress occurrence (Stone & Nicolas, 1995; Winkel et al., 1997). In addition to temperature and water supply, crop growth can be affected by other environmental factors (e.g., atmospheric CO₂ concentration and nitrogen supply; Rogers et al., 1996; de Oliveira et al., 2012; Shi et al., 2017) and non-environmental factors (e.g., genotype; Eller et al., 2020; Jiang et al., 2022; Wang et al., 2022).

Grain growth requires not only carbon but also nitrogen (Sinclair & de Wit, 1975). Thus, the concepts of source and sink cannot be applied merely to carbon assimilates, but should also include nitrogen (Martre et al., 2003; Triboi et al., 2003; Shao et al., 2021). While grain nitrogen comes partially from the post-anthesis nitrogen uptake, the remobilization of the pre-anthesis stored nitrogen in vegetative organs is known as the main source, and accounts for 50–100%, of the final grain nitrogen (Papkosta & Gagianas, 1991; Gebbing & Schnyder, 1999; Kichey et al., 2007; Shao et al., 2021), depending on species, genotype and growth conditions. Nonetheless, relatively little information is available on the responses of nitrogen source-sink relationships to environmental variables. Previous studies reported that environmental factors could influence nitrogen accumulation and remobilization (Palta et al., 1994; Barbottin et al., 2005). However, other studies suggested that environmental changes, such as global dimming (Shao et al., 2021) and elevated temperature and elevated CO₂ (Wang et al., 2019, 2020; Guo et al., 2022), would not significantly influence nitrogen source-sink relationships or alter amounts of grain nitrogen (protein) in cereals like wheat. Further systematic analyses are needed to reveal how environmental variables influence nitrogen budget in crops.

Wheat is one of the most important staple crops, annually producing more than 770 million tons of grains (FAOSTAT, 2022) and providing ~20% calories and protein in the human diet globally (Tilman et al., 2011; Shiferaw et al., 2013). Optimizing source-sink relationships is critical to improve wheat grain/nitrogen yield by ensuring a larger proportion of photo-assimilates/nitrogen to the sink, particularly under adverse conditions. Numerous studies have documented the effects of various factors on the grain-filling process in wheat. Yet, probably due to the lack of accurate methodologies, few studies simultaneously compared source and sink during grain filling at crop scale. A method developed by Yin et al. (2009) and Shi et al. (2017) can quantify the source-sink relationships for both biomass and nitrogen during the post-anthesis phase, a key period determining final grain yield for cereals (Yang et al., 2008). This method

relies on data for the post-anthesis time course of dry mass for both total aboveground and grain, and its advantages have been discussed (Yin et al., 2021). The method has been applied to several major annual crops (Shi et al., 2017; Wei et al., 2018; Shao et al., 2021; Zhang et al., 2022), for identifying genotypic or environmental factors that affect post-anthesis source-sink relationships.

Here, we used this method to analyze a large data set of biomass and nitrogen dynamics during the post-anthesis period in six wheat genotypes grown under a total of 62 contrasting temperature, water, and nitrogen regimes across 13 independent experiments conducted in semi-controlled conditions under natural sunlight at INRAE, France. By making use of this large data set, we aim at quantifying changes in wheat post-anthesis source and sink parameters under varying environmental regimes and providing an overview of wheat post-anthesis source-sink relationships under various environmental regimes. Such analyses would allow quantification of how contributions of remobilized pre-anthesis vs produced post-anthesis assimilates to grain growth can be affected by heat, WD and low nitrogen supply (LN), and how genotypes differ in their strategies for coping with adverse environments.

2 Materials and methods

2.1 Semi-controlled field experiments

We analyzed a data set from 13 experiments conducted in the (harvest) years of 1991, 1993, 1994, 1995, 1996, 1997, 1998, 1999, 2000, 2001, 2002, 2007 and 2014 (coded hereafter as EXP followed by year). Five winter wheat genotypes, Thésée (in EXP1991, EXP1993, EXP1994, EXP1995, EXP1996, EXP1997, and EXP1998), Renan (in EXP1999 and EXP2002), Récital (EXP2000, EXP2001, EXP2002, and EXP2007), Arche (in EXP2002), and Tamaro (in EXP2002), and a spring wheat line, SxB049 (in EXP2014) were grown. The latter was derived from a cross between the CIMMYT elite spring wheat genotypes Seri and Babax, and has been shown to better tolerate HT and WD, compared with its parents and sister lines (Pinto et al., 2010) (see Fig. 1 for all treatment abbreviations). All experiments were conducted at Clermont-Ferrand, France (45°47' N, 3°10' E, 329 m elevation) in the Crop Climate Control and Gas Exchange Measurement (C3-GEM) platform.

In all experiments, plants were grown in 2-m² steel containers with 0.5-m depth, filled with a 2:1 (v: v) mixture of black soil and peat. Seeds were sown in November in most experiments (except in EXP1995 and EXP2014; see Supplementary Table S1 for detailed sowing date for each experiment) at 2.5 cm from the soil surface with a density of 578 seeds m⁻², resulting in 329 to 634 plants m⁻² at anthesis (within each experiment, plant densities were similar among treatments). The high plant density inhibited the development of axillary tillers which helped synchronize the development of the crops within and between the containers. The anthesis dates for most experiments were in May, regardless of genotype (Table S1). Except for those cases where low nitrogen (LN) regimes were applied (see later), to avoid any nutrient deficiency, plants were fertilized several times at different growth stages and received a total of 15 to 33 g N m⁻² (Table S1). Plants were irrigated (in addition to receiving precipitation), whenever needed to maintain the soil water content above 80% of field capacity, except those regimes with WD (see later). For temperature treatments (see later), between 1 day before anthesis to 9 days after anthesis (DAA; depending on experiment and treatment; Fig. 1), each individual steel containers were transferred from outside ambient conditions to a soil-plant-atmosphere-research chamber with a closed air circulation. Chambers were covered by transparent polyethylene films where air temperature could be precisely controlled and natural precipitation could be excluded, allowing different temperature and water regimes to be applied (Triboï et al., 1996). The solar radiation inside chambers was ~70% of that outside. Additionally, for other soil WD regimes without temperature manipulations (see later), the steel containers were transferred under a mobile rain-out shelter.

2.2 Environmental regimes

The descriptions of the temperature, WD and LN regimes for all experiments are summarized Fig. 1 and are described in Table S1. The treatment codes include the final harvest year, genotype names, growth temperature regimes, and specific regimes, including heat shocks (HS), WD, elevated air CO₂ concentration (eCO₂) and LN. Arrows (→) indicate there was a temperature change from the original temperature (on the right of the arrow) to a new temperature (on the left of the arrow). Overall, the treatments in these experiments were divided into three factor groups, that is, *Temperature*, *Water* and *Genotype*. Within the *Temperature* group, experiments were

designed to investigate the effects of either long-term changes in temperature during the post-anthesis period ($T_{\text{post-anthesis}}$) or short-term extremely high temperatures (i.e., heat shocks; HS) on source-sink relationships during the post-anthesis period. A brief description of the experiment groups is given below.

Long-term change in $T_{\text{post-anthesis}}$: Treatments in this group were to explore the effects of either elevated (HT) or lowered (LT) $T_{\text{post-anthesis}}$ (Figs S1 and S4). Due to the complexity of the temperature regimes, they were divided into three subgroups: (i) *high growth temperature*, including both constant and fluctuating (i.e., the temperature inside the enclosure chamber followed the outside ambient temperature with a fixed difference); (ii) *diurnal thermal variability* (i.e., contrasting day/night temperature); (iii) *change in fluctuating growth temperature* during the grain-filling period:

- *High growth temperature:* in EXP1991 and EXP2000, constant high growth temperature regimes (28/20°C and 28/15°C for day/night in EXP1991 and EXP2000, respectively) were applied after anthesis.
- *Diurnal thermal variability:* in EXP1993 and EXP1996, three different day/night temperature regimes were applied after anthesis: 18/10°C (control), 34/10°C, and 28/20°C. In EXP1993, there was another regime, in which the 28/20°C temperature conditions were combined with elevated atmospheric CO₂ (eCO₂; 700 ppm, compared to 380 ppm for the other treatments). In EXP2014, four different day/night temperature regimes were applied to the spring wheat line SxB049: 21/15°C applied from 3 DAA to maturity (control), 22/20°C applied from 3 DAA to maturity, 29/23°C applied between 3 days and 12 DAA (i.e., endosperm cell division phase) and then 21/15°C until maturity, and 33/27°C applied between 3 days and 12 DAA and then 21/15°C until maturity. In EXP1995, a constant 28/20°C day/night temperature regime was implemented between 9 and 14 DAA, and then temperature was increased to 34/10°C until maturity.
- *Change in fluctuating growth temperature:* in EXP1994, five fluctuating temperature regimes relative to ambient air temperature were applied: (i) outside ambient temperature (Out°C; control); (ii) Out°C plus 5°C ('Out+5°C'); (iii) 'Out+5°C' until 18 DAA and then Out°C plus 10°C ('Out+10°C') until maturity ('Out+5°C→Out+10°C'); (iv) 'Out+10°C' until 16 DAA and then 'Out+5°C' until maturity ('Out+10°C→Out+5°C'); and (v) Out°C minus 5°C ('Out-5°C'). In EXP1997, two temperature regimes were applied in two chambers,

respectively: ‘Out+10°C’ until 22 DAA with 2 days of HS at 40°C for 4 h at 13 and 14 DAA, then day/night temperature was controlled at 34/20°C until maturity; ‘Out–5°C’ until 37 DAA, then day/night temperature was controlled at 18/10°C until maturity (for this regime, 34/10°C was applied in one of the chambers after 37 DAA; see Table S1). For the ‘Out+10°C’ regime in EXP1994 and in EXP1997, except during the two days of HS, temperature was controlled below 35°C and 34°C, respectively; and for the ‘Out–5°C’ regime in EXP1994 and EXP1997 the temperature was controlled above of 5°C.

Short-term extremely high temperature (HS): In this group, three experiments (EXP2001, EXP2007, EXP2000) explored the effects of HS during the post-anthesis period, and whether the effects depend on the timing of HS (Figs S1 and S4). In EXP2000, plants were grown at ‘Out–5°C’ until 21 DAA, after which the temperature regime was changed to a constant day/night temperature of 18/10°C. In EXP2001 and EXP2007, after anthesis all plant stands were maintained at a constant day/night temperature of 18/10°C and 21/14°C, respectively. Then HS were applied during the early-grain filling (HS1), mid-grain filling (HS2) and/or late-grain filling period (HS3). In EXP2001, HS, imposing 38°C for 4 h (between 10:00 and 14:00 solar time) during a day of 20 °C for the remaining hours, was applied for four consecutive days from 7 to 10 DAA (‘18/10°C HS1’), or from 18 to 21 DAA (‘18/10°C HS2’). In EXP2007, HS, 38–40°C imposed for 4 h (between 12:00 and 16:00 solar time) during a day of 21 °C for the remaining hours, was applied for four consecutive days from 8 to 11 DAA (‘21/14°C HS1’), from 23 to 26 DAA (‘21/14°C HS2’), and for both periods (‘21/14°C HS12’). In EXP2000, HS, 38°C imposed in two consecutive days for 4 h (between 11:30 and 14:30 solar time) on the first day and 6 h (between 10:15 and 16:15) on the second day, was applied starting 30 DAA (‘18/10°C HS3’). The rate of heating or cooling before and after the heat shocks was 4 to 9°C h⁻¹.

Water: In this group, three experiments (EXP2001, EXP1999 and EXP1998) were included to explore the effects of WD on source-sink relationship (Figs S2 and S5). We assessed whether or not the effects of pre- and post-anthesis WD and the interactions between WD and HT. In EXP2001, water was withheld from 7 to 21 DAA, with day/night temperature controlled at 18/10°C. EXP1999 aimed at analyzing WD by HT interactions. Day/night temperature was controlled at 18/10°C and 28/20°C starting 9 DAA under WW and WW conditions. The WD

regimes were applied by withholding water from 3 DAA. In EXP1998, there were two sub-experiments. In the first sub-experiment, after anthesis two temperature settings relative to outside ambient temperature were applied in four containers ('Out+5°C' and 'Out-5°C'); for each temperature setting, one container was well-irrigated and the other was subjected to WD treatment starting 0 DAA. In the second sub-experiment, plants of five containers were grown under outside ambient temperature; one container was well-irrigated (control), and a WD treatment was applied in the other four containers during the pre-anthesis period (water withheld from 28 days before anthesis until anthesis, WD1), the post-anthesis period (water withheld from 0 DAA to maturity, WD2), both the post- and post-anthesis periods (WD12), and from mid-grain filling to maturity (water withheld from 11 DAA to maturity, WD3). The total irrigation amount in each treatment in all the WD experiments is given in Table S1.

Genotype: EXP2002 was conducted to investigate the genetic variability in the responses of source-sink relationship under different post-anthesis growth conditions. Four winter wheat genotypes (Récital, Arche, Renan, Tamaro) with contrasted ratio of leaf area index to grain number (Martre et al., 2003), which is a proxy of the sink-source ratio (Figs S3 and S6), were grown under outside ambient temperature and under WW (control), WD, and LN regimes, and under constant day/night temperature controlled at 28/20°C (HT). In the WD regime, water withheld from 7 days before anthesis and 2 DAA to maturity, depending on the anthesis date of each genotype, and in the LN regime no nitrogen was applied after tillering stage.

2.3 Plant sampling and data collection

Plants were sampled every 2 to 9 days between anthesis and ripeness maturity. On each sampling date plants were collected on $0.2 \times 1.0 \text{ m}^2$ starting from the north side of the plant stands. The plants were individualized and counted, and one to three replicates of 20 plants each were analyzed separately. Stems, leaf laminae, chaffs, and grains of each subsample were separated, and their dry mass was determined after drying to constant mass in a forced air oven at 80°C. Total nitrogen concentration of oven-dried samples was determined by the Kjeldahl digestion method using a Kjeltac 2300 analyzer (Foss Tecator AB, Hoeganaes, Sweden) between 1991 and 2002, and by the Dumas combustion method using a FlashEA 19 1112 N/Protein analyzer (Thermo Electron Corp., Waltham, MA, USA) in 2007 and 2014.

2.4 Quantifying post-anthesis source-sink relationships

We quantified post-anthesis source-sink relationships in terms of either carbon or nitrogen, using the method developed by Yin et al. (2009) and Shi et al. (2017). Following their guideline, we used dry biomass data to analyze carbon source-sink relationships, as carbon fraction in biomass does not change significantly among plant organs in crops like wheat, nor among growth conditions (Penning de Vries et al., 1989). In this method, sink parameters are estimated from the time course of grain dry mass or nitrogen during the grain filling period, whereas source parameters are estimated from the dynamics of the total aboveground biomass or nitrogen mass (including senesced materials) during the same period. Thus, the “source” in the method refers to biomass accumulated, or nitrogen taken up, only during the post-anthesis period; but as described later, by comparing the post-anthesis “source” supply with the post-anthesis grain “sink” demand, the method does give an estimate of the contribution to grain growth of remobilized pre-anthesis assimilates (which usually are also considered as a “source” to grain growth). In the method, the dynamics of both post-anthesis source and sink are described by a set of equations. To distinguish parameters, we use the subscripts ‘si’ and ‘so’ to indicate sink and source, respectively, throughout the text and equations. Symbols of all model parameters are defined in Table 1. Moreover, wherever appropriate, we use the subscripts ‘M’ and ‘N’ to indicate dry mass and nitrogen, respectively.

(i) *Estimation of sink-related parameters:* The dynamic data of either grain dry mass (g m^{-2}) or grain nitrogen (g m^{-2}) per unit ground area collected during the post-anthesis period can be described by a determinate sigmoid growth function (Yin et al., 2003):

$$W_{\text{si}} = \begin{cases} (W_{\text{x,si}} - W_{\text{b,si}}) \left(1 + \frac{t_{\text{e,si}} - t}{t_{\text{e,si}} - t_{\text{m,si}}}\right) \left(\frac{t - t_{\text{b}}}{t_{\text{e,si}} - t_{\text{b}}}\right)^{\frac{t_{\text{e,si}} - t_{\text{b}}}{t_{\text{e,si}} - t_{\text{m,si}}}} + W_{\text{b,si}} & \text{if } t_{\text{b}} \leq t < t_{\text{e,si}} \\ W_{\text{x,si}} & \text{if } t \geq t_{\text{e,si}} \end{cases} \quad (1)$$

where t represents DAA, W_{si} is observed grain dry mass or nitrogen mass per unit ground area at time t , $W_{\text{b,si}}$ is the initial grain dry mass or nitrogen mass per unit ground area at anthesis (t_{b}), $W_{\text{x,si}}$ is the maximum grain dry mass or nitrogen mass per unit ground area when grain filling ends ($t_{\text{e,si}}$), and $t_{\text{m,si}}$ is the time when the maximum grain-filling rate is achieved (Fig. 2A). Here, we set $t_{\text{b}} = 0$, as in earlier studies (Yin et al., 2009; Shi et al., 2017; Wei et al., 2018; Shao et al., 2021), and we also set $W_{\text{b,si}} = 0$ as grain dry mass or nitrogen mass is expected to be close to zero

at anthesis (i.e., the dry mass and nitrogen of ovules was neglected). After the parameters of Equation (1) were estimated by fitting the curves to the measured data, daily sink strength (Fig. 2B), that is, the rate of change in grain dry mass or nitrogen mass per unit area can be calculated by the differential form of Equation (1), i.e.:

$$\text{Sink strength} = \begin{cases} s_{\max, \text{si}} \left(\frac{t_{e, \text{si}} - t}{t_{e, \text{si}} - t_{m, \text{si}}} \right) \left(\frac{t - t_b}{t_{m, \text{si}} - t_b} \right)^{\frac{t_{m, \text{si}} - t_b}{t_{e, \text{si}} - t_{m, \text{si}}}} & \text{if } t < t_{e, \text{si}} \\ 0 & \text{if } t \geq t_{e, \text{si}} \end{cases} \quad (2)$$

where $s_{\max, \text{si}}$ is the maximum sink strength ($\text{g m}^{-2} \text{day}^{-1}$; i.e., the maximum grain filling rate) at the time $t_{m, \text{si}}$ (DAA), which can be calculated as (Yin et al., 2009)

$$s_{\max, \text{si}} = (W_{x, \text{si}} - W_{b, \text{si}}) \left[\frac{2t_{e, \text{si}} - t_{m, \text{si}} - t_b}{(t_{e, \text{si}} - t_{b, \text{si}})(t_{e, \text{si}} - t_{m, \text{si}})} \right] \left(\frac{t_{m, \text{si}} - t_b}{t_{e, \text{si}} - t_b} \right)^{\frac{t_{m, \text{si}} - t_b}{t_{e, \text{si}} - t_{m, \text{si}}}} \quad (3)$$

Further, the mean sink strength (\bar{s}_{si} , $\text{g m}^{-2} \text{day}^{-1}$; i.e., the mean grain filling rate) during the whole grain filling period can be calculated as:

$$\bar{s}_{\text{si}} = \frac{W_{x, \text{si}} - W_{b, \text{si}}}{t_{e, \text{si}} - t_b} \quad (4)$$

and the total sink demand ($S_{\text{tot, si}}$, g m^{-2}) during the whole grain filling period can be calculated as (Yin et al., 2021):

$$S_{\text{tot, si}} = W_{x, \text{si}} - W_{b, \text{si}} \quad (5)$$

Parameters described above could be applied to both dry mass and nitrogen data.

(ii) *Estimation of source-related parameters:* The source activity ($\text{g m}^{-2} \text{day}^{-1}$; i.e., the rate of change of aboveground biomass or nitrogen mass per unit ground area) declines during the grain filling period (Fig. 2C), and this can be described by a reversed sigmoid model (Yin et al., 2009):

$$\text{Source activity} = \begin{cases} s_{\max, \text{so}} \left[1 - \left(1 + \frac{t_{e, \text{so}} - t}{t_{e, \text{so}} - t_{m, \text{so}}} \right) \left(\frac{t}{t_{e, \text{so}}} \right)^{\frac{t_{e, \text{so}}}{t_{e, \text{so}} - t_{m, \text{so}}}} \right] & \text{if } t < t_{e, \text{so}} \\ 0 & \text{if } t \geq t_{e, \text{so}} \end{cases} \quad (6)$$

where $t_{e, \text{so}}$ is DAA when the source activity has decreased to zero, $t_{m, \text{so}}$ is DAA when the rate of decrease of source activity is maximum, and $s_{\max, \text{so}}$ is the maximum source activity at the onset of the grain filling ($\text{g m}^{-2} \text{day}^{-1}$; i.e., the maximum rate of change of aboveground biomass or

nitrogen mass per unit ground area). Integrating Equation (6) over time gives the following expression for the time course of aboveground biomass or nitrogen mass per unit ground area (g m^{-2}), W_{so} :

$$W_{\text{so}} = \begin{cases} s_{\text{max,so}} t \left[1 - \left(1 - \frac{t}{3t_{\text{e,so}} - 2t_{\text{m,so}}} \right) \left(\frac{t}{t_{\text{e,so}}} \right)^{\frac{t_{\text{e,so}}}{t_{\text{e,so}} - t_{\text{m,so}}}} \right] + W_{\text{b,so}} & \text{if } t < t_{\text{e,so}} \\ W_{\text{x,so}} & \text{if } t \geq t_{\text{e,so}} \end{cases} \quad (7)$$

Fitting Equation (7) to the data for the time course of aboveground biomass or nitrogen mass per unit ground area (Fig. 2D) gives an estimate of $s_{\text{max,so}}$ in addition to $t_{\text{e,so}}$ and $t_{\text{m,so}}$. By setting $t = t_{\text{e,so}}$, one can obtain from Equation (7) that $W_{\text{x,so}} - W_{\text{b,so}} = s_{\text{max,so}} \frac{t_{\text{e,so}}^2}{3t_{\text{e,so}} - 2t_{\text{m,so}}}$ (Yin et al., 2009).

Combining this with Equation (7) gives an alternative equation for W_{so} :

$$W_{\text{so}} = \begin{cases} \left[(W_{\text{x,so}} - W_{\text{b,so}}) \frac{(3t_{\text{e,so}} - 2t_{\text{m,so}})t}{t_{\text{e,so}}^2} \right] \left[1 - \left(1 - \frac{t}{3t_{\text{e,so}} - 2t_{\text{m,so}}} \right) \left(\frac{t}{t_{\text{e,so}}} \right)^{\frac{t_{\text{e,so}}}{t_{\text{e,so}} - t_{\text{m,so}}}} \right] + W_{\text{b,so}} & \text{if } t < t_{\text{e,so}} \\ W_{\text{x,so}} & \text{if } t \geq t_{\text{e,so}} \end{cases} \quad (8)$$

where $W_{\text{b,so}}$ is the aboveground biomass or nitrogen per unit ground area at anthesis (g m^{-2}), $W_{\text{x,so}}$ is the maximum aboveground biomass or nitrogen mass per unit ground area at the end of the growing season (g m^{-2}).

The mean source activity (\bar{s}_{so} , $\text{g m}^{-2} \text{ day}^{-1}$) during the whole grain filling period can be calculated as:

$$\bar{s}_{\text{so}} = \frac{W_{\text{x,so}} - W_{\text{b,so}}}{t_{\text{e,so}} - t_{\text{b}}} \quad (9)$$

and the total source supply ($S_{\text{tot,so}}$, g m^{-2}) during the whole grain-filling period can be calculated as:

$$S_{\text{tot,so}} = W_{\text{x,so}} - W_{\text{b,so}} \quad (10)$$

(iii) *Statistical analysis of source-sink balance*: The post-anthesis source/sink ratio was defined as $S_{\text{tot,so}}/S_{\text{tot,si}}$ and the post-anthesis source-sink difference was calculated as $(S_{\text{tot,so}} - S_{\text{tot,si}})$. The common procedure for estimating source and sink parameters was to fit Equation (8) and Equation (1) separately, which would fail to statistically test whether or not $S_{\text{tot,so}}$ (i.e., $W_{\text{x,so}} - W_{\text{b,so}}$) and $S_{\text{tot,si}}$ (i.e., $W_{\text{x,si}} - W_{\text{b,si}}$) are balanced. To solve this problem, following Shao et al. (2021), we introduced dummy variables (Z_1 and Z_2) and defined them using binary values in

such a way that $Z_1=1$ and $Z_2=0$ corresponds to the source whereas $Z_1=0$ and $Z_2=1$ represents the sink:

$$W = Z_1 W_{so} + Z_2 W_{si} \quad (11)$$

By combining Equations (1) and (8) with Equation (11), all parameters in Equations (1) and (8) can be estimated simultaneously in a single procedure by fitting observed data of the time course of both W_{so} and W_{si} (the full model) (see an example in Supplementary Protocol S1 on how dummy-variable values were given). Then, we set a null hypothesis (H_0) that $S_{tot,so}$ mathematically equals $S_{tot,si}$ (i.e., post-anthesis source and sink are balanced), which gives:

$$W_{x,so} = W_{x,si} - W_{b,si} + W_{b,so} \quad (12)$$

We incorporated Equation (12) into the fitting procedure, thereby removing $W_{x,so}$ from parameters to be fitted (reduced model). By comparing the residual sum of squares and degrees of freedom between the two sets of fitting for the full model and the reduced model, we performed an F -test to test whether or not the total post-anthesis source and sink are significantly different. An insignificant F -value at $P = 0.05$ meant to accept the H_0 , i.e., post-anthesis source and sink are balanced.

(iv) *Quantifying remobilization*: While the method, as stated earlier, does not explicitly include pre-anthesis assimilates as a “source” term, it does allow us to quantify the required remobilization of pre-anthesis assimilates/nitrogen to support grain (sink) growth. The contribution of pre-anthesis (RE , %) carbon assimilates or nitrogen to the sink is given by:

$$RE = \frac{S_{tot,si} - S_{tot,so}}{S_{tot,si}} \times 100 \quad (13)$$

It should be noted that Equation (13) works best when $S_{tot,si} \geq S_{tot,so}$. When $S_{tot,si} > S_{tot,so}$, then post-anthesis production does not suffice and a remobilization of pre-anthesis reserves is required and the required RE (%) is as calculated by Equation (13). When $S_{tot,si} = S_{tot,so}$, then post-anthesis production just suffices for the grain demand and the required RE is 0%. When $S_{tot,si} < S_{tot,so}$, however, the term $(S_{tot,si} - S_{tot,so})$ and RE are negative, meaning that the post-anthesis source supply has a surplus relative to sink demand and there is no remobilization of

pre-anthesis assimilates needed. The absolute value of this difference can be interpreted as the surplus that will add to the existing pre-anthesis reserves.

The framework as described was to analyze data for post-anthesis aboveground as well as grain dynamics in order to quantify the post-anthesis source-sink relationships and pre-anthesis reserve contribution (RE , %) to grain growth. It assumes that grains are the predominant aboveground sink during grain filling. Strictly speaking, when stems and leaves are also sinks to some extent, the calculated RE , if zero or even negative, does not mean that remobilization did not occur at all. Similarly, if RE is above zero, it does not mean that the actual total remobilization is that number. But our calculated RE (%) conclusively quantifies the “net” remobilization that is needed to contribute to grain growth. Also, the method could ideally be applied to estimate the source parameters using the *whole-plant* biomass or N data (that includes roots). However, measuring belowground dynamics is practically infeasible at a large scale. Environmental variables may alter root dynamics during the post-anthesis phase. If this indeed occurred, our estimated $S_{\text{tot.so}}$ would represent either the gross (post-anthesis production plus remobilization from roots if roots “export”) or the net (post-anthesis production minus partitioning to roots if roots “import”) post-anthesis assimilate supply for aboveground growth. In either case, the term $(S_{\text{tot.si}} - S_{\text{tot.so}})$ does not change if grains are indeed the predominant sink for available aboveground assimilates during grain filling. As a result, RE (referring to the contribution of pre-anthesis aboveground reserves to grains) would become somewhat smaller if roots “export” and somewhat larger if roots “import”.

2.5 Curve fitting

Non-linear curve fitting procedures were implemented using the GAUSS method in PROC NLIN of the statistical software SAS version 9.4 (SAS Institute Inc, Cary, NC, USA). The SAS codes can be found in the Supplementary Protocol S1. We performed the fitting, using pooled data of individual replicates to obtain estimates of parameters which are most reliable for representing treatment-specific parameters (which in fact are close to the mean of replicated estimates but have better statistical predictions of all data points than the mean). In the cases where over-fitting occurred, we fixed the value of $t_{e.so}$ at the first data point where a plateau (the maximum value) was observed. $W_{b.so}$ represents the initial aboveground biomass or nitrogen mass at anthesis, and its values is assumed to be identical among treatments that were applied after anthesis. Thus, to

minimize errors, in each year, for those treatments applied after anthesis, curve fitting was first performed within each treatment, and then data were re-fitted by fixing $W_{b,so}$ at the mean value of $W_{b,so}$ across treatments.

In EXP1997, although day/night temperatures were changed to 18/10°C and 34/10°C after ‘Out–5°C’ at 37 DAA in two chambers, respectively, the data showed little difference; therefore, data collected from the two plant stands with the same regime (‘Out+10°C→34/20°C’) or similar regimes (‘Out–5°C→18/10°C’ and ‘Out–5°C→34/10°C’) were pooled together to be fitted. In EXP2002, the aboveground biomass of Tamaro initially increased but later decreased after reaching a peak (around 400 to 500 ° Cd, depending on treatments), while at the same time the grain biomass was still increasing. The decreased aboveground biomass during later grain filling period resulted in very little aboveground biomass accumulation over the whole grain filling period. Similarly, the amount of aboveground nitrogen was relatively constant during the post-anthesis period. Thus, we assumed the total source supply for biomass or nitrogen during the post-anthesis period was zero for Tamaro.

3 Results

3.1 The model described well the dynamics of post-anthesis source and sink

By using the method developed by Yin et al. (2009) and Shi et al. (2017), we quantified post-anthesis source, sink and their relationships in 13 independent experiments (see Fig. 1 for experimental regimes). As stated earlier, source supply for grain filling is usually defined as the sum of the pre-anthesis stored carbohydrates and the post-anthesis produced assimilates (Asseng et al., 2017; Reynolds et al., 2022). Here, based on our modeling framework, we parameterized source only based on the biomass produced or nitrogen accumulated after anthesis. As illustrated in Fig. 2, the dynamics of post-anthesis sink and source were well described by the model [Equations (1) and (8)], with an average R^2 of 0.943 ± 0.017 ($n = 62$) for biomass and of 0.922 ± 0.020 ($n = 39$) for nitrogen.

3.2 Relations for biomass

Both $S_{\text{tot.si.M}}$ and $S_{\text{tot.so.M}}$ varied with experiments and environmental regimes (Fig. 3A). On average $S_{\text{tot.si.M}}$ was ~10% higher than $S_{\text{tot.so.M}}$, indicating that overall, the remobilization of pre-anthesis reserves was required. However, the calculated average RE for biomass varied from –19% to 100% (depending on experiments and environmental regimes) with a mean value of 22% (Figs S1B, S2B, S3B). The plot of Fig. 4A appeared to identify a value of $S_{\text{tot.si.M}}$ (~950 g m⁻²). Below this value, pre-anthesis stored carbon assimilates increasingly contributed to the grain biomass. Above the value, post-anthesis photo-assimilates were in a slight excess of the demand for grain filling, as shown by negative values of RE calculated by Equation (13).

Both short-term heat shocks (HS; 4 h at 38°C for 2-4 days) and long-term temperature elevation (HT) reduced $S_{\text{tot.so.M}}$ and $S_{\text{tot.si.M}}$, but in general HT had larger effects than HS (Fig. S1A). The impacts of HT on $S_{\text{tot.so.M}}$ and $S_{\text{tot.si.M}}$ varied among regimes. For instance, $S_{\text{tot.so.M}}$ and $S_{\text{tot.si.M}}$ were more reduced by 34/10°C than by 28/20°C (EXP1993 and EXP1996 in Fig. S1A), even though $T_{\text{post-anthesis}}$ was identical between the two temperature regimes. Elevated CO₂ slightly mitigated the negative impact of 28/20°C on $S_{\text{tot.so.M}}$ but not that on $S_{\text{tot.si.M}}$ (EXP1993 in Fig. S1A). Also, high night temperature (22/20°C) did not affect $S_{\text{tot.so.M}}$ and $S_{\text{tot.si.M}}$ (EXP2014 in Fig. S1A). Two to four days of HS did not change relative values of $S_{\text{tot.so.M}}$ and $S_{\text{tot.si.M}}$, regardless of the timing when HS were applied (Fig. 3A; Fig. S1A). Likewise, HT had limited impacts on the differences between $S_{\text{tot.so.M}}$ and $S_{\text{tot.si.M}}$ (Fig. 3A). For example, in many cases (EXP1993, EXP1994, EXP1995, EXP1997, EXP2000 and EXP2014), the $S_{\text{tot.so.M}} - S_{\text{tot.si.M}}$ difference was not significant, and thus RE for biomass was low (Fig. S1A,B).

WD and LN, particularly WD, had profound impacts on the relative differences between $S_{\text{tot.so.M}}$ and $S_{\text{tot.si.M}}$, with $S_{\text{tot.so.M}}$ being significantly lower than $S_{\text{tot.si.M}}$; therefore, high RE for biomass were observed in these regimes (Fig. 4A; Figs S2B and S3B). The impact of WD on $S_{\text{tot.so.M}}$ and $S_{\text{tot.si.M}}$ depended on the timing of WD. For example, in EXP1998, compared with WD2 (water withheld from 0 DAA to maturity), WD1 (water withheld from 28 days before anthesis to anthesis) had greater impacts on $S_{\text{tot.so.M}}$ and $S_{\text{tot.si.M}}$ (Fig. S2A). Moreover, the impact of WD on biomass was larger under HT than under ambient temperature. In EXP1999, $S_{\text{tot.so.M}}$ and $S_{\text{tot.si.M}}$ was reduced by 42% and 27% under WD regimes compared with the well-watered (WW) regime, respectively; and the combination of HT (28/15°C) and WD reduced $S_{\text{tot.so.M}}$ and

$S_{\text{tot.si.M}}$ by 78% and 55%, respectively (Fig. S2A). Similar results were also found in EXP1998 (Fig. S2A).

Post-anthesis biomass source and sink parameters were also genotype-dependent. Under ambient control conditions (CK), Arche, Récital, Renan and Tamaro showed contrasting $S_{\text{tot.so.M}}/S_{\text{tot.si.M}}$ ratios, with Arche having the highest ratio while Tamaro having the lowest ratio (Fig. S3A), which confirmed results observed in the field (Martre et al., 2003). Although HT, WD and LN all reduced $S_{\text{tot.so.M}}$ and $S_{\text{tot.si.M}}$, their impacts varied among genotypes. For instance, WD decreased $S_{\text{tot.si.M}}$ for Arche, Récital and Renan by 30%, 42%, and 45%, respectively. However, under WD, $S_{\text{tot.so.M}}$ for Arche remained relatively high (it decreased by only 20% compared to CK), which was not the case for Récital and Renan ($S_{\text{tot.so.M}}$ decreased by 48% and 80% for Récital and Renan, respectively). These resulted in a decrease in the $S_{\text{tot.so.M}}/S_{\text{tot.si.M}}$ ratio for Récital and Renan and in an increased ratio for Arche (Fig. S3A). Additionally, RE for biomass were always observed for Récital, Renan and Tamaro, regardless of growth conditions, while for Arche RE was substantial only under HT and LN (Fig. S3B).

3.3 Relations for nitrogen

Like $S_{\text{tot.si.M}}$ and $S_{\text{tot.so.M}}$, both $S_{\text{tot.si.N}}$ and $S_{\text{tot.so.N}}$ varied with the studied factors and environmental regimes (Fig. 3A). In all regimes, $S_{\text{tot.si.N}}$ were significantly higher than $S_{\text{tot.so.N}}$ (Figs S4A, S5A, S6A), and overall $S_{\text{tot.si.N}}$ was as high as 215% of $S_{\text{tot.so.N}}$ (Fig. 3B). Thus, high RE values for nitrogen were observed in all cases, ranging from 18% to 100% with an average of 63% (Figs 4B, S4B, S5B, S6B).

Environmental regimes (e.g., HT, HS and WD) did not markedly affect the relationships between $S_{\text{tot.so.N}}$ and $S_{\text{tot.si.N}}$, but genotype and its interaction with environmental regimes did (Fig. S6). For instance, HT decreased both $S_{\text{tot.so.N}}$ and $S_{\text{tot.si.N}}$ for Récital by 90% and 27%, respectively, and for Arche by 62% and 35%, respectively (Fig. S6A); whereas for Renan, HT did not significantly decrease $S_{\text{tot.so.N}}$ and $S_{\text{tot.si.N}}$ (Fig. S6A). WD markedly decreased $S_{\text{tot.so.N}}$ and $S_{\text{tot.si.N}}$ for Renan (by 27% and 32%, respectively), but had limited impacts on those for Arche where $S_{\text{tot.so.N}}$ even increased by 40% under WD (Fig. S6A).

3.4 Temperature responses of estimated parameters

For biomass, under WW and non-limiting nitrogen (HN) regimes, both $S_{\text{tot.so.M}}$ and $t_{e.\text{so.M}}$ decreased with increasing $T_{\text{post-anthesis}}$ (Fig. 5A,B). In most WD and LN regimes the values of both $S_{\text{tot.so.M}}$ and $t_{e.\text{so.M}}$ were lower than expected from their temperature response. $\bar{s}_{\text{so.M}}$ was not significantly correlated with the $T_{\text{post-anthesis}}$, and averaged $18 \text{ g m}^{-2} \text{ day}^{-1}$ for WW and HN regimes and $12 \text{ g m}^{-2} \text{ day}^{-1}$ for WD and LN regimes (Fig. 5C). As for the sink parameters, $S_{\text{tot.si.M}}$ and $t_{e.\text{si.M}}$ were negatively correlated with $T_{\text{post-anthesis}}$ under WW and HN regimes (Fig. 5D,E). In most WD and LN regimes $S_{\text{tot.si.M}}$ was lower than expected from its temperature response. $t_{e.\text{si.M}}$ was less reduced in WD and LN regimes than $S_{\text{tot.si.M}}$ (Fig. 5D,E). $\bar{s}_{\text{si.M}}$ was not significantly correlated with $T_{\text{post-anthesis}}$ (Fig. 5F), and averaged $20 \text{ g m}^{-2} \text{ day}^{-1}$ for WW and HN regimes and $14 \text{ g m}^{-2} \text{ day}^{-1}$ for WD and LN regimes. *F* test analysis showed that under WW and HN regimes $S_{\text{tot.so.M}}$ and $S_{\text{tot.si.M}}$ (Fig. 5A,D) had similar response to $T_{\text{post-anthesis}}$. The difference between $S_{\text{tot.so.M}}$ and $S_{\text{tot.si.M}}$ (Fig. 5G), the ratio of $S_{\text{tot.so.M}}$ to $S_{\text{tot.si.M}}$ (Fig. 5H), and *RE* for biomass (Fig. 5I) were not significantly correlated with $T_{\text{post-anthesis}}$, irrespective of water and nitrogen regimes. *RE* for biomass averaged 15% for WW and HN regimes and 41% for WD and LN regimes (Fig. 5I).

For nitrogen parameters, $S_{\text{tot.so.N}}$ and $S_{\text{tot.si.N}}$, and their difference and ratio, were not significantly correlated with $T_{\text{post-anthesis}}$, regardless of water regimes (Fig. 6A,D,G,H). Both $t_{e.\text{so.N}}$ (Fig. 6B) and $t_{e.\text{si.N}}$ (Fig. 6E) decreased as $T_{\text{post-anthesis}}$ increased under both WW and WD regimes, and WD slightly modified the temperature responses of $t_{e.\text{so.N}}$ and $t_{e.\text{si.N}}$. $\bar{s}_{\text{si.N}}$, but not $\bar{s}_{\text{so.N}}$, showed significantly positive correlation ($P < 0.01$) with $T_{\text{post-anthesis}}$ under WW and HN regimes (Fig. 6C,F).

4 Discussion

With a quantitative analysis of post-anthesis biomass and nitrogen accumulation for several wheat genotypes grown in a large set of experiments, we were able to systematically investigate to what extent post-anthesis source and sink parameters for biomass and nitrogen can be affected by temperature, water, and nitrogen regimes, and genotype.

4.1 High temperatures had little impact on post-anthesis biomass relationships

Pooling the results across all experiments gave an overall picture of post-anthesis biomass source supply vs sink demand across factors and environmental regimes (Fig. 3A). The relationship shown in Fig. 4A identified a grain yield value (equivalent to $S_{\text{tot.si.M}}$ being about 950 g m^{-2}), at and above which (mostly under CK and LT conditions) no remobilization of pre-anthesis stored assimilates was required. Under adverse conditions (mainly under WD and LN conditions) when grain yield was lower than $\sim 950 \text{ g m}^{-2}$, post-anthesis source supply was insufficient in support of sink demand, leading to an increasing contribution of remobilized pre-anthesis assimilates to grain yield (Fig. 4A).

However, there was little effect of HS on total post-anthesis source supply ($S_{\text{tot.so.M}}$) and sink demand ($S_{\text{tot.si.M}}$) in most cases. Instead, it was the average post-anthesis temperature ($T_{\text{post-anthesis}}$) that played a predominate role. Our results suggested that $S_{\text{tot.so.M}}$ and $S_{\text{tot.si.M}}$ decreased similarly with increasing $T_{\text{post-anthesis}}$ under WW and HN regimes (Fig. 5A,D), and these decreases were determined more by the post-anthesis durations ($t_{e.\text{so.M}}$ and $t_{e.\text{si.M}}$; Fig. 5B,E) than by the mean rates of source supply ($\bar{s}_{\text{so.M}}$) and sink demand ($\bar{s}_{\text{si.M}}$) (Fig. 5C,F). These results were in line with the common observation that the acceleration of phenology is the primary driver of the negative impact of rising temperatures on crop production, because the shortened growing period will result in less time for carbon assimilation and grain filling, eventually leading to yield loss (Wardlaw & Moncur, 1995; Zhao et al., 2007; Liu et al., 2014; Asseng et al., 2015, 2019). HS did not lead to obvious deviations in the temperature response curves of source and sink parameters. Moreover, the relatively constant source-supply rate ($\bar{s}_{\text{so.M}}$) across $T_{\text{post-anthesis}}$ may be partially attributed from the low sensitivity of canopy photosynthetic rate to increasing air temperatures, due to the cooling effect by evapotranspiration, at canopy scale under WW conditions (Webber et al., 2017). It could also be a result from the remobilization of carbohydrates from belowground to aboveground under adverse conditions during grain filling (Palta et al., 1994), or could be explained by other factors, such as the in-season variations of solar radiation (Asseng et al., 2017; Shao et al., 2021) and diurnal temperature variations (Asseng et al., 2015). The relatively constant sink-demand rate ($\bar{s}_{\text{si.M}}$) at different $T_{\text{post-anthesis}}$ is in contrast with previous experimental observations at single-plant level where wheat grain filling rate was affected by temperature (Yin et al., 2009). The relatively smaller variations of $\bar{s}_{\text{si.M}}$ (Fig.

5F) compared with $\bar{s}_{so,M}$ (Fig. 5C) could have been due to compensations by pre-anthesis assimilate remobilization.

The temperature responses of total post-anthesis source supply ($S_{tot,so,M}$) and sink demand ($S_{tot,si,M}$) were downward shifted under WD and LN regimes (Fig. 5A,D). Yet, the extent of the shift was stronger for $S_{tot,so,M}$ than for $S_{tot,si,M}$, as a result of higher remobilization ($RE\%$) under WD and LN regimes. Like high temperatures, WD accelerates senescence (Evans, 1993; Farooq et al., 2014) and decreases photosynthesis (Liu et al., 2019; Wei et al., 2020, 2022; Fang et al., 2023). However, in contrast to some previous findings that WD hardly affects or slightly increases grain filling rate (Nicolas et al., 1984; Yang & Zhang, 2006), here, the rates (both $\bar{s}_{so,M}$ and $\bar{s}_{si,M}$) were suppressed across $T_{post-anthesis}$ under WD or LN regimes, resulting in the lower biomass accumulation ($S_{tot,so,M}$ and $S_{tot,si,M}$) (Fig. 5A-F).

Under natural field conditions heat and drought often concurrently occur (i.e., compound stresses), leading to difficulties to identify the separate impacts of heat and drought (Lesk et al., 2022). Consequently, the impact of heat stress may be overestimated. Here, our results revealed that WD and the combined WD and HT exerted a more profound impact on wheat biomass sink-source relationships than HT alone (Fig. 3A). This is in line with our previous finding at leaf scale that post-anthesis drought exerts a greater impact on photosynthesis than post-anthesis heat (Fang et al., 2023).

4.2 Post-anthesis nitrogen relationships hardly responded to temperature and water regimes

Unlike the source of grain biomass that is mainly produced after anthesis, the source of grain nitrogen mainly comes from the nitrogen uptake before anthesis (Papkosta & Gagianas, 1991; Gebbing & Schnyder, 1999; Shao et al., 2021), which was also supported by our study. On average, RE across all environmental regimes and genotypes were 22% for biomass (Fig. 4A) and 63% for nitrogen (Fig. 4B). In line with the higher RE for nitrogen, the mean rate of grain nitrogen accumulation ($\bar{s}_{si,N}$) was higher than the mean rate of post-anthesis nitrogen uptake ($\bar{s}_{so,N}$) (Fig. S7D). Our results suggest that the discrepancy between the rates of grain nitrogen demand and post-anthesis nitrogen uptake was independent of the post-anthesis duration (Fig. S7B).

Some earlier studies showed that wheat nitrogen fluxes were influenced by environmental changes (Palta et al., 1994; Barbottin et al., 2005). However, while our study could not identify the effect of LN due to the lack of data, we found that total post-anthesis nitrogen uptake ($S_{\text{tot.so.N}}$), total grain nitrogen accumulation ($S_{\text{tot.si.N}}$) and their difference or ratio were insensitive to $T_{\text{post-anthesis}}$ and water supply (Fig. 6A,D,G,H), and RE for nitrogen was roughly constant across $T_{\text{post-anthesis}}$ and water regimes (Fig. 6I). This was also in agreement with previous findings that nitrogen partitioning is unaffected by post-anthesis heat and drought in wheat (Triboï et al., 2003), and that nitrogen relationships during grain filling are little affected by shading applied after stem-elongation in wheat (Shao et al., 2021). In fact, most regimes in our study were imposed after anthesis (Fig. 1), when crops had already taken up sufficient nitrogen for filling grains, implying that environmental changes during the post-anthesis period would have limited impacts on the amount of available nitrogen for remobilization, and thus on total grain nitrogen accumulation ($S_{\text{tot.si.N}}$). As a result, we also observed an increased $\bar{s}_{\text{si.N}}$, mainly due to an increased remobilization of nitrogen, that could have compensated for the decreased grain-nitrogen accumulation duration ($t_{e.\text{si.N}}$) with increasing $T_{\text{post-anthesis}}$ (Fig. 6E,F). A similar compensation between the rate and duration of grain nitrogen accumulation for wheat in response to post-anthesis temperature was observed by Dupont et al. (2006).

While we observed that total grain nitrogen accumulation ($S_{\text{tot.si.N}}$) positively correlated with total grain biomass ($S_{\text{tot.si.M}}$) (Fig. S8B), this did not necessarily imply that they respond similarly to environmental variables (Panozzo et al., 1999; Dupont et al., 2006). High temperatures and WD reduced $S_{\text{tot.si.M}}$ and average final grain dry mass (Fig. 5D; Fig. S9A), but did not significantly affect $S_{\text{tot.si.N}}$ (Fig. 6D) and average final nitrogen mass per grain (Fig. S9E), leading to an increase in grain nitrogen concentration (Fig. S9D). Many previous studies (e.g., Kimball et al., 2001, Yin et al., 2009) also showed this. Given that high temperatures and WD mostly occur during the post-anthesis period in most wheat-growing regions (Asseng et al., 2019), our results implied that a future warmer and drier climate may not lower grain nitrogen/protein concentration of wheat. This was in agreement with the advocacy of recent studies that the combined elevated temperature and elevated CO_2 would not result in lower grain nutritional quality for wheat and rice (Wang et al., 2019, 2020; Guo et al., 2022), but was in contrast to earlier reports (e.g., Myers et al. (2014) who only considered the elevated- CO_2 effect) that climate change threatens grain quality.

of reserve assimilates under drought and the combination of drought and heat appeared to be important for increasing productivity under climate change. Also, our study suggested that warmer and drier future climates may not threaten the quality of wheat grain in terms of protein concentration (Fig. S9D). Finally, to reduce the uncertainty in assessing future climate change impacts, efforts to understand the interactions of multiple (non-)environmental factors (e.g., temperature \times water \times CO₂ \times fertilization \times genotype), rather than the impact of a single or merely two factors, are needed (Mittler, 2006; Suzuki et al., 2014; Webber et al., 2022).

Accepted Manuscript

Author Contribution

X.Y. and P.M. conceived the study; C.G. and P.M. conceived the experimentation; L.F. and P.M. sorted out raw data archives; X.Y. designed the model methods; L.F. conducted analyses and wrote the draft; P.C.S., C.G., X.Y. and P.M. revised the manuscript.

Conflict of Interest

The authors have no conflicts to declare.

Funding Sources

None

Data Availability

The data that support the findings of this study are openly available at Dryad Digital Repository (doi:10.5061/dryad.9ghx3ffrw).

Accepted Manuscript

References

- Asseng, S., Ewert, F., Martre, P., Rötter, R. P., Lobell, D. B., Cammarano, D., Kimball, B.A., Ottman, M.J., Wall, G.W., White, J.W., Reynolds, M.P., Alderman, P.D., Prasad, P.V.V., Aggarwal, P.K., Anothai, J., Basso, B., Biernath, C., Challinor, A.J., De Sanctis, G., Doltra, J., Fereres, E., Garcia-Vila, M., Gayler, S., Hoogenboom, G., Hunt, L.A., Izaurrealde, R.C., Jabloun, M., Jones, C.D., Kersebaum, K.C., Koehler, A.-K., Müller, C., Naresh Kumar, S., Nendel, C., O'Leary, G., Olesen, J.E., Palosuo, T., Priesack, E., Eyshi Rezaei, E., Ruane, A.C., Semenov, M.A., Shcherbak, I., Stöckle, C., Stratonovitch, P., Streck, T., Supit, I., Tao, F., Thorburn, P.J., Waha, K., Wang, E., Wallach, D., Wolf, J., Zhao, Z. & Zhu, Y. (2015). Rising temperatures reduce global wheat production. *Nature Climate Change*, 5(2), 143-147.
- Asseng, S., Kassie, B. T., Labra, M. H., Amador, C., & Calderini, D. F. (2017). Simulating the impact of source-sink manipulations in wheat. *Field Crops Research*, 202, 47-56.
- Asseng, S., Martre, P., Maiorano, A., Rötter, R. P., O'Leary, G. J., Fitzgerald, G. J., Girousse, C., Motzo, R., Giunta, F., Babar, M.A., Reynolds, M.P., Kheir, A.M.S., Thorburn, P.J., Waha, K., Ruane, A.C., Aggarwal, P.K., Ahmed, M., Balkovič, J., Basso, B., Biernath, C., Bindi, M., Cammarano, D., Challinor, A.J., De Sanctis, G., Dumont, B., Eyshi Rezaei, E., Fereres, E., Ferrise, R., Garcia-Vila, M., Gayler, S., Gao, Y., Horan, H., Hoogenboom, G., Izaurrealde, R.C., Jabloun, M., Jones, C.D., Kassie, B.T., Kersebaum, K.-C., Klein, C., Koehler, A.-K., Liu, B., Minoli, S., San Martin, M.M., Müller, C., Kumar, S.N., Nendel, C., Olesen, J.E., Palosuo, T., Porter, J.R., Priesack, E., Ripoche, D., Semenov, M.A., Stöckle, C., Stratonovitch, P., Streck, T., Supit, I., Tao, F., Van der Velde, M., Wallach, D., Wang, E., Webber, H., Wolf, J., Xiao, L., Zhang, Z., Zhao, Z., Zhu, Y. & Ewert, F. (2019). Climate change impact and adaptation for wheat protein. *Global Change Biology*, 25(1), 155-173.
- Barbottin, A., Lecomte, C., Bouchard, C., & Jeuffroy, M. H. (2005). Nitrogen remobilization during grain filling in wheat: genotypic and environmental effects. *Crop Science*, 45(3), 1141-1150.
- Barnabás, B., Jäger, K., & Fehér, A. (2008). The effect of drought and heat stress on reproductive processes in cereals. *Plant, Cell & Environment*, 31(1), 11-38.
- Chenu, K., Porter, J. R., Martre, P., Basso, B., Chapman, S. C., Ewert, F., Bindi, M. & Asseng, S. (2017). Contribution of crop models to adaptation in wheat. *Trends in Plant Science*, 22(6), 472-490.
- de Oliveira, E. D., Bramley, H., Siddique, K. H., Henty, S., Berger, J., & Palta, J. A. (2012). Can elevated CO₂ combined with high temperature ameliorate the effect of terminal drought in wheat? *Functional Plant Biology*, 40(2), 160-171.
- Dingkuhn, M., Luquet, D., Fabre, D., Muller, B., Yin, X. and Paul, M., 2020. The case for improving crop carbon sink strength or plasticity for a CO₂-rich future. *Current Opinion in Plant Biology*, 56, 259-272.
- Dupont FM, Hurkman WJ, Vensel WH, Tanaka C, Kothari KM, Chung OK, Altenbach SB. 2006. Protein accumulation and composition in wheat grains: effects of mineral nutrients and high temperature. *European Journal of Agronomy*, 25, 96-107.
- Eller, F., Hyldgaard, B., Driever, S. M., & Ottosen, C. O. (2020). Inherent trait differences explain wheat cultivar responses to climate factor interactions: New insights for more robust crop modelling. *Global Change Biology*, 26(10), 5965-5978.
- Evans, L.T. (1993) *Crop Evolution, Adaptation and Yield*. Cambridge University Press, Cambridge, UK.

- Fang, L., Martre, P., Jin, K., Du, X., van der Putten, P. E., Yin, X., & Struik, P. C. (2023). Neglecting acclimation of photosynthesis under drought can cause significant errors in predicting leaf photosynthesis in wheat. *Global Change Biology*, 29(2), 505-521.
- FAOSTAT: FAO statist. databases (2022) <https://www.fao.org/faostat/en/#home>
- Farooq, M., Hussain, M., & Siddique, K. H. (2014). Drought stress in wheat during flowering and grain-filling periods. *Critical Reviews in Plant Sciences*, 33(4), 331-349.
- Gebbing, T., & Schnyder, H. (1999). Pre-anthesis reserve utilization for protein and carbohydrate synthesis in grains of wheat. *Plant Physiology*, 121(3), 871-878.
- Guo, X., Huang, B., Zhang, H., Cai, C., Li, G., Li, H., Zhang, Y., Struik, P.C., Liu, Z., Dong, M., Ni, R., Pan, G., Liu, X., Chen, W., Luo, W. & Yin, X. (2022). T- FACE studies reveal that increased temperature exerts an effect opposite to that of elevated CO₂ on nutrient concentration and bioavailability in rice and wheat grains. *Food and Energy Security*, 11(1), e336.
- Jiang, D., Mulero, G., Bonfil, D. J., & Helman, D. (2022). Early or late? The role of genotype phenology in determining wheat response to drought under future high atmospheric CO₂ levels. *Plant, Cell & Environment*, 45(12), 3445-3461.
- Kichey, T., Hirel, B., Heumez, E., Dubois, F., & Le Gouis, J. (2007). In winter wheat (*Triticum aestivum* L.), post-anthesis nitrogen uptake and remobilisation to the grain correlates with agronomic traits and nitrogen physiological markers. *Field Crops Research*, 102(1), 22-32.
- Kimball, B. A., Morris, C. F., Pinter Jr, P. J., Wall, G. W., Hunsaker, D. J., Adamsen, F. J., LaMorte, R.L., Leavitt, S.W., Thompson, T.L., Matthias, A.D. & Brooks, T.J. (2001). Elevated CO₂, drought and soil nitrogen effects on wheat grain quality. *New Phytologist*, 150(2), 295-303.
- Lesk, C., Anderson, W., Rigden, A., Coast, O., Jägermeyr, J., McDermid, S., Davis, K.F. & Konar, M. (2022). Compound heat and moisture extreme impacts on global crop yields under climate change. *Nature Reviews Earth & Environment*, 3(12), 872-889.
- Liu, B., Liu, L., Tian, L., Cao, W., Zhu, Y., & Asseng, S. (2014). Post- heading heat stress and yield impact in winter wheat of China. *Global Change Biology*, 20(2), 372-381.
- Liu, J., Hu, T., Fang, L., Peng, X., & Liu, F. (2019). CO₂ elevation modulates the response of leaf gas exchange to progressive soil drying in tomato plants. *Agricultural and Forest Meteorology*, 268, 181-188.
- Martre P, Porter JR, Jamieson PD, Triboi E. 2003. Modeling grain nitrogen accumulation and protein composition to understand the sink/source regulations of nitrogen remobilization for wheat. *Plant Physiology* 133, 1959-1967.
- Mittler, R. (2006). Abiotic stress, the field environment and stress combination. *Trends in Plant Science*, 11(1), 15-19.
- Myers, S. S., Zanobetti, A., Kloog, I., Huybers, P., Leakey, A. D.B., Bloom, A. J., Carlisle, E., Dietterich, L. H., Fitzgerald, G., Hasegawa, T., Holbrook, N. M., Nelson, R. L., Ottman, M. J., Raboy, V., Sakai, H., Sartor, K. A., Schwartz, J., Seneweera, S., Tausz, M., & Usui, Y. (2014). Increasing CO₂ threatens human nutrition. *Nature*, 510(7503), 139-142.
- Nicolas, M. E., Gleadow, R. M., & Dalling, M. J. (1984). Effects of drought and high temperature on grain growth in wheat. *Functional Plant Biology*, 11(6), 553-566.
- Palta, J. A., Kobata, T., Turner, N. C., & Fillery, I. R. (1994). Remobilization of carbon and nitrogen in wheat as influenced by postanthesis water deficits. *Crop Science*, 34(1), 118-124.

- Panozzo JF, Eagles HA. 1999. Rate and duration of grain filling and grain nitrogen accumulation of wheat cultivars grown in different environments. *Australian Journal of Agricultural Research*, 50, 1007-1015.
- Papakosta, D. K., & Gagianas, A. A. (1991). Nitrogen and dry matter accumulation, remobilization, and losses for Mediterranean wheat during grain filling. *Agronomy Journal*, 83(5), 864-870.
- Penning de Vries, F.W.T., Jansen, D.M., ten Berge, H.F.M., & Bakema, A., 1989. Simulation of ecophysiological processes of growth in several annual crops. IRRI, Los Banos and Pudoc, Wageningen.
- Pinto, R. S., Reynolds, M. P., Mathews, K. L., McIntyre, C. L., Olivares-Villegas, J. J., & Chapman, S. C. (2010). Heat and drought adaptive QTL in a wheat population designed to minimize confounding agronomic effects. *Theoretical and Applied Genetics*, 121, 1001-1021.
- Reynolds, M. P., Slafer, G. A., Foulkes, J. M., Griffiths, S., Murchie, E. H., Carmo-Silva, E., ... & Flavell, R. B. (2022). A wiring diagram to integrate physiological traits of wheat yield potential. *Nature Food*, 3(5), 318-324.
- Rogers, G. S., Milham, P. J., Gillings, M., & Conroy, J. P. (1996). Sink strength may be the key to growth and nitrogen responses in N-deficient wheat at elevated CO₂. *Functional Plant Biology*, 23(3), 253-264.
- Schapendonk, A. H. C. M., Xu, H. Y., Van Der Putten, P. E. L., & Spiertz, J. H. J. (2007). Heat-shock effects on photosynthesis and sink-source dynamics in wheat (*Triticum aestivum* L.). *NJAS-Wageningen Journal of Life Sciences*, 55(1), 37-54.
- Shao, L., Liu, Z., Li, H., Zhang, Y., Dong, M., Guo, X., Zhang, H., Huang, B., Ni, R., Li, G., Cai, C., Chen, W., Luo, W. & Yin, X. (2021). The impact of global dimming on crop yields is determined by the source–sink imbalance of carbon during grain filling. *Global Change Biology*, 27(3), 689-708.
- Shi, W., Xiao, G., Struik, P. C., Jagdish, K. S., & Yin, X. (2017). Quantifying source-sink relationships of rice under high night-time temperature combined with two nitrogen levels. *Field Crops Research*, 202, 36-46.
- Shiferaw, B., Smale, M., Braun, H. J., Duveiller, E., Reynolds, M., & Muricho, G. (2013). Crops that feed the world 10. Past successes and future challenges to the role played by wheat in global food security. *Food Security*, 5, 291-317.
- Sinclair, T. R., & de Wit, C. T. (1975). Photosynthate and nitrogen requirements for seed production by various crops. *Science*, 189(4202), 565-567.
- Stone, P. J., & Nicolas, M. E. (1995). Effect of timing of heat stress during grain filling on two wheat varieties differing in heat tolerance. I. Grain growth. *Functional Plant Biology*, 22(6), 927-934.
- Suzuki, N., Rivero, R. M., Shulaev, V., Blumwald, E., & Mittler, R. (2014). Abiotic and biotic stress combinations. *New Phytologist*, 203(1), 32-43.
- Tilman, D., Balzer, C., Hill, J., & Befort, B. L. (2011). Global food demand and the sustainable intensification of agriculture. *Proceedings of the National Academy of Sciences*, 108(50), 20260-20264.
- Triboi, E., Martre, P., & Triboi- Blondel, A. M. (2003). Environmentally- induced changes in protein composition in developing grains of wheat are related to changes in total protein content. *Journal of Experimental Botany*, 54(388), 1731-1742.

- Tribouï E, Tribouï-Blondel A, Martignac M, Falcimagne R (1996) Experimental device for studying post-anthesis canopy functioning in relation to grain quality. In: *Proc 4th European Society of Agronomy Congress, Amsterdam Academic Press, Wageningen, The Netherlands, pp68-69*. pp Page.
- Wang, J., Hasegawa, T., Li, L., Lam, S. K., Zhang, X., Liu, X., & Pan, G. (2019). Changes in grain protein and amino acids composition of wheat and rice under short- term increased [CO₂] and temperature of canopy air in a paddy from East China. *New Phytologist*, 222(2), 726-734.
- Wang, J., Li, L., Lam, S. K., Liu, X., & Pan, G. (2020). Responses of wheat and rice grain mineral quality to elevated carbon dioxide and canopy warming. *Field Crops Research*, 249, 107753.
- Wang, X., Li, X., Zhong, Y., Blennow, A., Liang, K., & Liu, F. (2022). Effects of elevated CO₂ on grain yield and quality in five wheat cultivars. *Journal of Agronomy and Crop Science*, 208(5), 733-745.
- Wardlaw, I. F., & Moncur, L. J. F. P. B. (1995). The response of wheat to high temperature following anthesis. I. The rate and duration of kernel filling. *Functional Plant Biology*, 22(3), 391-397.
- Webber, H., Martre, P., Asseng, S., Kimball, B., White, J., Ottman, M., Wall, G.W., De Sanctis, G., Doltra, J., Grant, R., Kassie, B., Maiorano, A., Olesen, J.E., Ripoche, D., Eyshi Rezaei, E., Semenov, M.A., Stratonovitch, P. & Ewert, F. (2017). Canopy temperature for simulation of heat stress in irrigated wheat in a semi-arid environment: A multi-model comparison. *Field Crops Research*, 202, 21-35.
- Webber, H., Rezaei, E. E., Ryo, M., & Ewert, F. (2022). Framework to guide modeling single and multiple abiotic stresses in arable crops. *Agriculture, Ecosystems & Environment*, 340, 108179.
- Wei, H., Meng, T., Li, X., Dai, Q., Zhang, H., & Yin, X. (2018). Sink-source relationship during rice grain filling is associated with grain nitrogen concentration. *Field Crops Research*, 215, 23-38.
- Wei, Z., Abdelhakim, L. O. A., Fang, L., Peng, X., Liu, J., & Liu, F. (2022). Elevated CO₂ effect on the response of stomatal control and water use efficiency in amaranth and maize plants to progressive drought stress. *Agricultural Water Management*, 266, 107609.
- Wei, Z., Fang, L., Li, X., Liu, J., & Liu, F. (2020). Effects of elevated atmospheric CO₂ on leaf gas exchange response to progressive drought in barley and tomato plants with different endogenous ABA levels. *Plant and Soil*, 447(1), 431-446.
- Winkel, T., Renno, J. F., & Payne, W. A. (1997). Effect of the timing of water deficit on growth, phenology and yield of pearl millet (*Pennisetum glaucum* (L.) R. Br.) grown in Sahelian conditions. *Journal of Experimental Botany*, 48(5), 1001-1009.
- Yang, J., & Zhang, J. (2006). Grain filling of cereals under soil drying. *New Phytologist*, 169(2), 223-236.
- Yang, J., Zhang, J., Liu, K., Wang, Z., & Liu, L. (2006). Abscisic acid and ethylene interact in wheat grains in response to soil drying during grain filling. *New Phytologist*, 171(2), 293-303.
- Yang, W., Peng, S., Dionisio-Sese, M. L., Laza, R. C., & Visperas, R. M. (2008). Grain filling duration, a crucial determinant of genotypic variation of grain yield in field-grown tropical irrigated rice. *Field Crops Research*, 105(3), 221-227.
- Yin, X., & Struik, P. C. (2017). Can increased leaf photosynthesis be converted into higher crop mass production? A simulation study for rice using the crop model GECROS. *Journal of Experimental Botany*, 68(9), 2345-2360.

- Yin, X., Guo, W., & Spiertz, J. H. (2009). A quantitative approach to characterize sink–source relationships during grain filling in contrasting wheat genotypes. *Field Crops Research*, *114*(1), 119-126.
- Yin, X., Struik, P. C., & Goudriaan, J. (2021). On the needs for combining physiological principles and mathematics to improve crop models. *Field Crops Research*, *271*, 108254.
- Zhang, S., Wang, H., Fan, J., Zhang, F., Cheng, M., Yang, L., Ji, Q. & Li, Z. (2022). Quantifying source-sink relationships of drip-fertigated potato under various water and potassium supplies. *Field Crops Research*, *285*, 108604.
- Zhao, C., Liu, B., Piao, S., Wang, X., Lobell, D. B., Huang, Y., Yao, Y., Bassu, S., Ciais, P., Durand, J.-L., Elliott, J., Ewert, F., Janssens, I.A., Li, T., Lin, E., Liu, Q., Martre, P., Müller, C., Peng, S., Peñuelas, J., Ruane, A.C., Wallach, D., Wang, T., Wu, D., Liu, Z., Zhu, Y., Zhu, Z., & Asseng, S. (2017). Temperature increase reduces global yields of major crops in four independent estimates. *Proceedings of the National Academy of sciences*, *114*(35), 9326-9331.
- Zhao, H., Dai, T., Jing, Q., Jiang, D., & Cao, W. (2007). Leaf senescence and grain filling affected by post-anthesis high temperatures in two different wheat cultivars. *Plant Growth Regulation*, *51*(2), 149-158.

Accepted Manuscript

Table 1. List of symbols of parameters of the source-sink model, and their definitions and units

Symbol	Definition	Unit
t	Days after anthesis	day
t_b	Anthesis date (denoted as days after anthesis, so, set as zero in the model)	day
$t_{m,si}$	Days after anthesis when the daily sink strength is maximum	day
$t_{e,si}$	Days after anthesis when the daily sink strength has decreased to zero. $t_{e,si,M}$ and $t_{e,si,N}$ represent $t_{e,si}$ for biomass and nitrogen, respectively	day
W_{si}	Observed grain dry mass or nitrogen mass per unit ground area	g m^{-2}
$W_{b,si}$	Initial grain dry mass or nitrogen mass at anthesis (set as zero in the model)	g m^{-2}
$W_{x,si}$	Maximum grain dry mass or nitrogen mass per unit of ground area	g m^{-2}
$S_{max,si}$	Maximum sink strength (i.e., maximum rate of grain filling)	$\text{g m}^{-2} \text{ day}^{-1}$
\bar{S}_{si}	Mean sink strength (i.e., mean grain-filling rate) of the whole grain filling period. $\bar{S}_{si,M}$ and $\bar{S}_{si,N}$ represent \bar{S}_{si} for biomass and nitrogen, respectively	$\text{g m}^{-2} \text{ day}^{-1}$
$S_{tot,si}$	Total sink demand of the whole grain filing period. $S_{tot,si,M}$ and $S_{tot,si,N}$ represent $S_{tot,si}$ for biomass and nitrogen, respectively	g m^{-2}
$t_{m,so}$	Days after anthesis when the daily source activity declines at a maximum rate	day
$t_{e,so}$	Days after anthesis when the daily source activity has decreased to zero. $t_{e,so,M}$ and $t_{e,so,N}$ represent $t_{e,so}$ for biomass and nitrogen, respectively	day
W_{so}	Observed aboveground biomass or nitrogen mass per unit ground area	g m^{-2}
$W_{b,so}$	Aboveground biomass or nitrogen mass per unit ground area at anthesis	g m^{-2}
$W_{x,so}$	Maximum aboveground biomass or nitrogen mass per unit ground area at the end of the grain filling	g m^{-2}
$S_{max,so}$	Maximum daily source activity, which is set to be achieved at the onset of grain filling	$\text{g m}^{-2} \text{ day}^{-1}$
\bar{S}_{so}	Mean source activity of the whole grain-filling period. $\bar{S}_{so,M}$ and $\bar{S}_{so,N}$ represent \bar{S}_{so} for biomass and nitrogen, respectively	$\text{g m}^{-2} \text{ day}^{-1}$
$S_{tot,so}$	Total source supply of the whole grain filling period. $S_{tot,so,M}$ and $S_{tot,so,N}$ represent $S_{tot,so}$ for biomass and nitrogen, respectively	g m^{-2}
RE	Contribution of remobilized pre-anthesis biomass (or nitrogen) needed to final grain dry biomass (or final grain nitrogen mass)	%

Figure 1. Schema of the temperature, water deficit, and low nitrogen regimes tested in the 13 experiments analyzed in this study. In EXP1994, EXP1995 and EXP2000, before the beginning of setpoint temperature, plants were grown at 18/10°C (day/night temperature) during the temperature control period. In EXP2000, before temperature regimes changed to 18/10°C, plants were grown at Out–5°C. Abbreviations and symbols: CK, control treatment; eCO₂, elevated air CO₂ concentration; Out°C, outside ambient temperature; Out+5°C, outside ambient temperature plus 5°C; Out+10°C, outside ambient temperature plus 10°C; Out–5°C, outside ambient temperature minus 5°C; HS, heat shock; WW, well-watered; WD, water deficit; LN, low nitrogen. HS1, HS2, HS12 and HS3 represent heat shocks during the early-grain filling period, the mid-grain filling period, and during both early- and mid-grain filling periods and during late-grain filling period, respectively. WD1, WD2, WD12 and WD3 represent water deficit stress occurring during the pre-anthesis period, the post-anthesis period, both pre- and post-anthesis periods, and during the late-grain filling period, respectively. Details and codes for experiments and treatments on the left are defined in Supplementary Table S1.

Figure 2. Example of the post-anthesis time course of the measured grain dry mass and total aboveground biomass per unit area and the resulting dynamics of daily sink strength and source activity during grain filling. (A) Time course of grain dry mass during the post-anthesis period as described by Equation (1). (B) Dynamic of resulting daily sink strength during the post-anthesis period as described by Equation (2). (C) Dynamic of daily source activity during the post-anthesis period as described by Equation (6). (D) Time course of aboveground biomass during the post-anthesis period as described by Equation (8). The symbols of the model parameters are defined in Table 1. All time variable or parameters are expressed as days after anthesis. Data used for this example illustration are for the winter wheat genotype Thésée grown under outside ambient temperature conditions (Out°C) in EXP1994. In (A) and (D), circles and errors bars are means ± s.e. of three replicates.

Figure 3. Relationships between post-anthesis source and sink. Total post-anthesis source supply ($S_{\text{tot,so}}$) and total sink demand ($S_{\text{tot,si}}$) for biomass (A) and nitrogen (B) are plotted for winter wheat cultivars grown under different temperature, water deficit, and low nitrogen regimes. The shaded area depicts the 95% confidence interval of the predictions. Dashed lines are the 1:1 relationship. The full lines represent regression equations (significant at $P < 0.001$). The bold number (%) above the regression equation in each panel is the average of y-axis relative to x-axis values across regimes. Data are for factors of ‘Temperature’ (long-term temperature changes and short-term heat shocks regimes; Figs S1 and S4), ‘Water’ (water supply regimes; Figs S2 and S5), and ‘Genotype’ (the wheat genotypes Thésée, Récital, Renan, Arche and Tamaro grown under high temperature, water deficit and low nitrogen regimes; Figs S3 and S6). CK, control treatment; LT, low growth temperature (Out–5°C); HT, high growth temperature; eCO₂, elevated air CO₂ concentration; HS, heat shock; WD, water deficit stress and LN, low nitrogen supply.

Figure 4. The required contribution (%) of remobilized pre-anthesis assimilates to grain growth (RE) versus grain sink demand. This is shown for biomass (A, where the x-axis is total grain biomass $S_{\text{tot,si,M}}$) and for nitrogen (B, where the x-axis is total grain nitrogen $S_{\text{tot,si,N}}$), based on the pooled results for winter wheat cultivars grown under different temperature, water deficit, and low nitrogen regimes. The shaded area depicts the 95% confidence interval of the predictions. The full lines represent regression equations (* and *** significant at $P < 0.05$ and 0.001, respectively). Dashed horizontal lines indicate the case when $RE = 0\%$, while the dashed vertical line in panel (A) identifies a value of $S_{\text{tot,si,M}}$, below which RE is $> 0\%$ and above which RE is $< 0\%$. The bold value in each panel is the mean RE across regimes. Symbols for experimental factors are identified as in Fig. 3. The extreme values of RE at 100% in panel (A) are for cv. Tamaro, which hardly accumulated aboveground biomass during the whole grain filling period such that its grain growth relied entirely on remobilized assimilates (see the text). As $S_{\text{tot,si,M}}$ and $S_{\text{tot,si,N}}$ decreased with increasing stress intensity, this figure suggests that the remobilization of pre-anthesis reserves became increasingly important for grain growth with increasing stress intensity, as discussed in the text.

Figure 5. Post-anthesis source and sink parameters for biomass (M) versus average daily temperature of the period. (A-C) Temperature responses of total source supply ($S_{\text{tot.so.M}}$), days after anthesis when the source activity has decreased to zero ($t_{e.\text{so.M}}$), and mean source activity ($\bar{s}_{\text{so.M}}$) for biomass. (D-F) Temperature responses of total sink demand ($S_{\text{tot.si.M}}$), days after anthesis when the daily sink strength has decreased to zero ($t_{e.\text{si.M}}$), and mean sink strength ($\bar{s}_{\text{si.M}}$) for biomass. (G-I) Temperature responses of the difference between $S_{\text{tot.so.M}}$ and $S_{\text{tot.si.M}}$, the ratio of $S_{\text{tot.so.M}}$ to $S_{\text{tot.si.M}}$, and the contribution of remobilized pre-anthesis assimilates to final grain dry mass (RE for biomass). Lines are linear regression fitted to the data for the well water and high nitrogen supply regimes and are shown only when significant at $P = 0.05$. *** indicates statistical significance at $P < 0.001$. The shaded area depicts the 95% confidence interval of the predictions for the conditions well-watered and high nitrogen supply regimes. WW, well-watered; WD, water deficit; HN, non-limiting nitrogen; LN, low nitrogen supply; HS, heat shock.

Figure 6. Post-anthesis source and sink parameters for nitrogen (N) versus average daily temperature of the period. (A-C) Temperature responses of total source supply ($S_{\text{tot.so.N}}$), days after anthesis when the source activity has decreased to zero ($t_{e.\text{so.N}}$), and mean source activity ($\bar{s}_{\text{so.N}}$) for nitrogen. (D-F) Temperature responses of total sink demand ($S_{\text{tot.si.N}}$), days after anthesis when the daily sink strength has decreased to zero ($t_{e.\text{si.N}}$), and mean sink strength ($\bar{s}_{\text{si.N}}$) for nitrogen. (G-I) Temperature responses of the difference between $S_{\text{tot.so.N}}$ and $S_{\text{tot.si.N}}$, the ratio of $S_{\text{tot.so.N}}$ to $S_{\text{tot.si.N}}$, and the contribution of remobilized pre-anthesis nitrogen to final grain nitrogen mass (RE for nitrogen). Lines are linear regression fitted to the data for the well water and high nitrogen supply regimes and are shown only when significant at $P = 0.05$. ** and *** indicate statistical significance at $P < 0.01$ and 0.001 , respectively. The shaded area depicts the 95% confidence interval of the predictions. WW, well-watered; WD, water deficit; HN, non-limiting nitrogen; HS, heat shock.

Accepted Manuscript

Figure 1

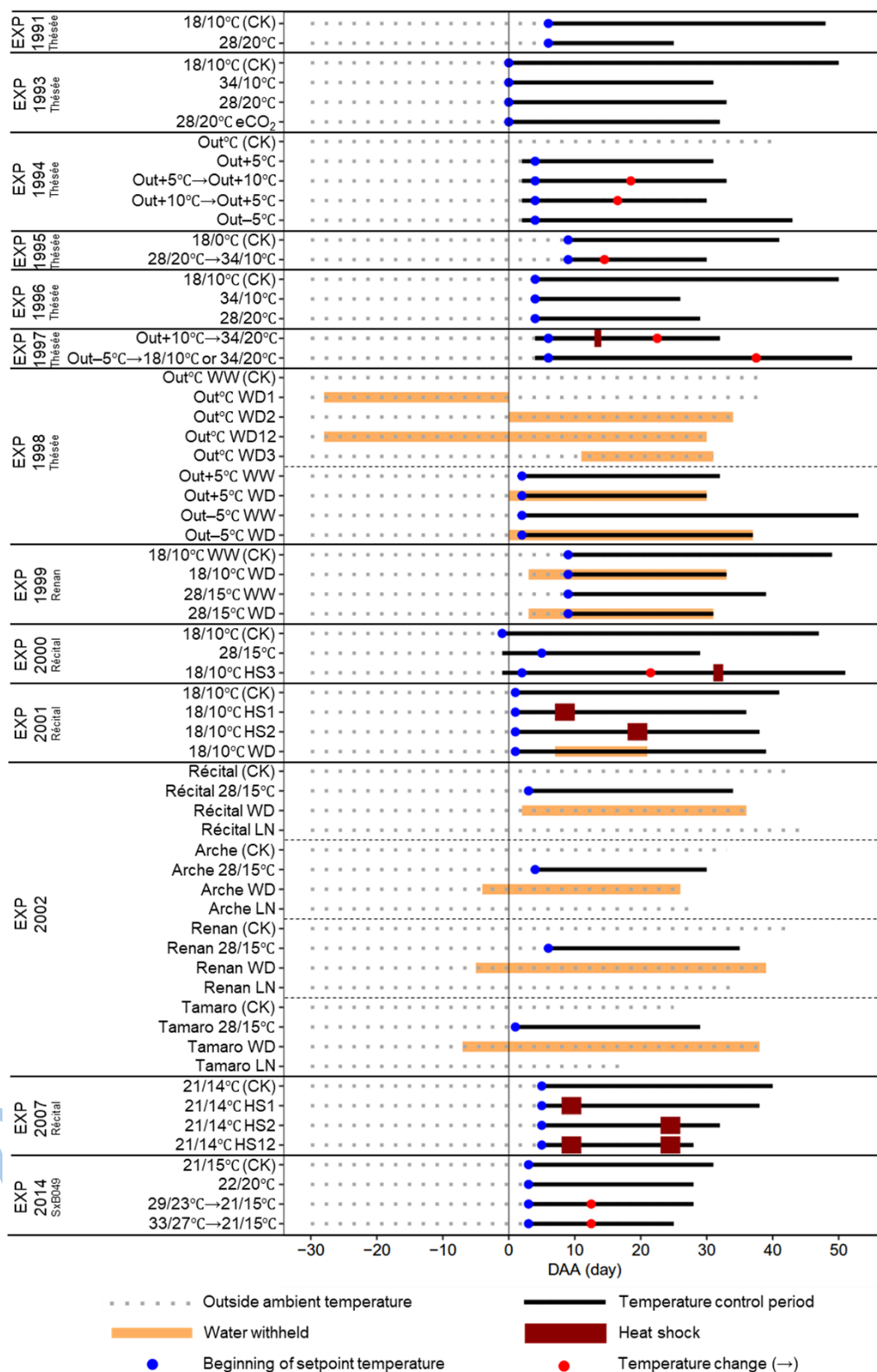
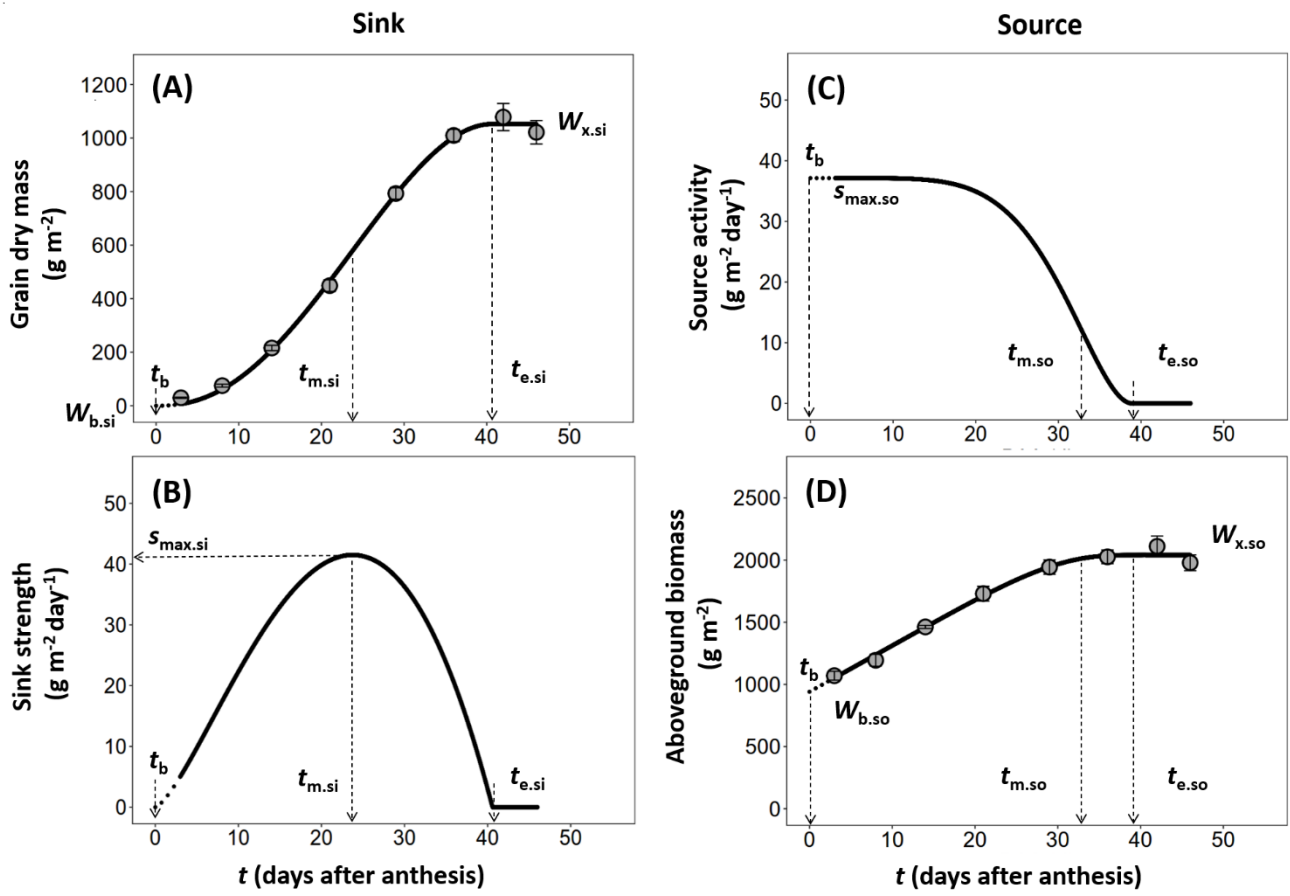


Figure 2



Accepted

Figure 3

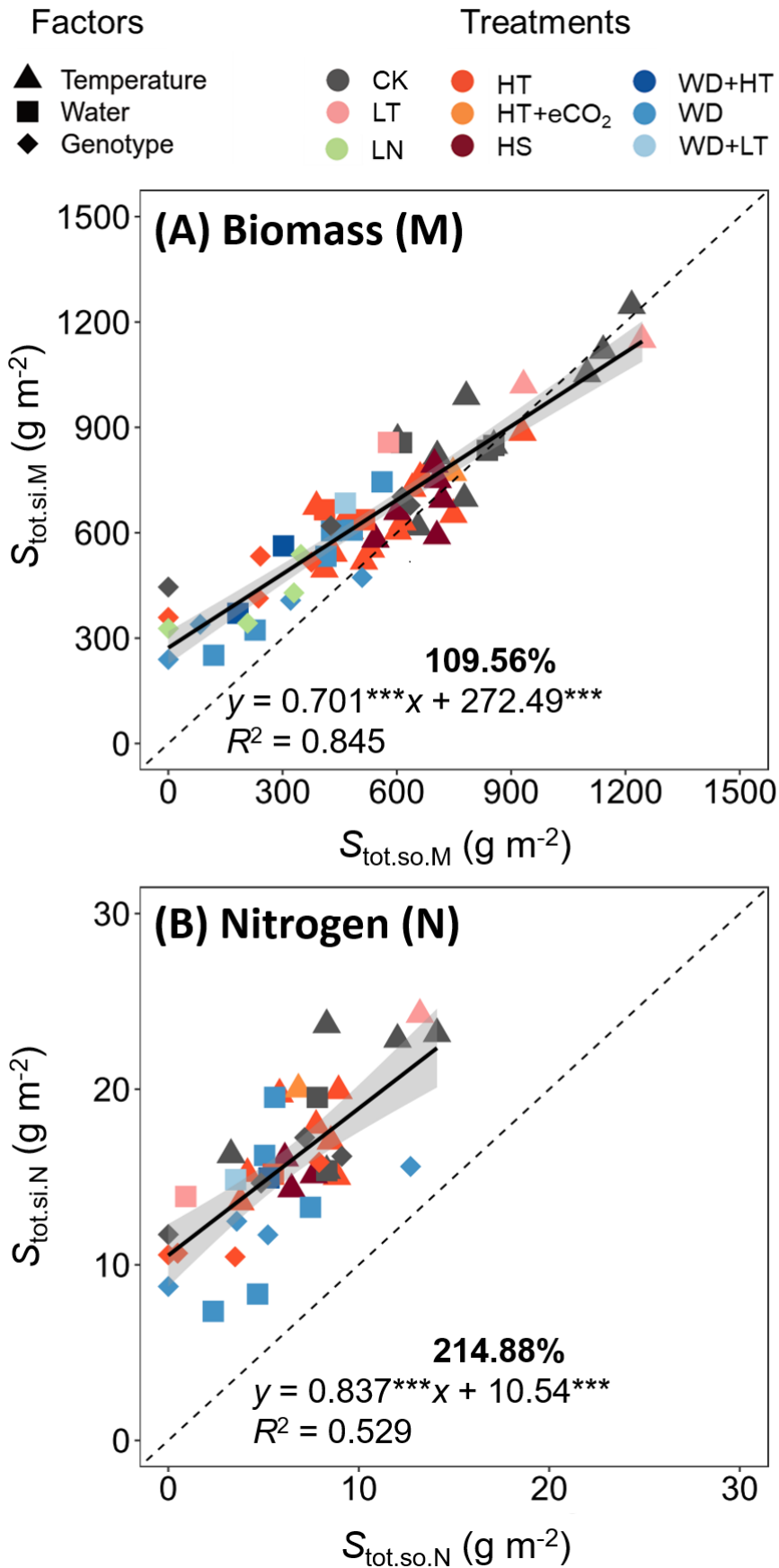


Figure 4

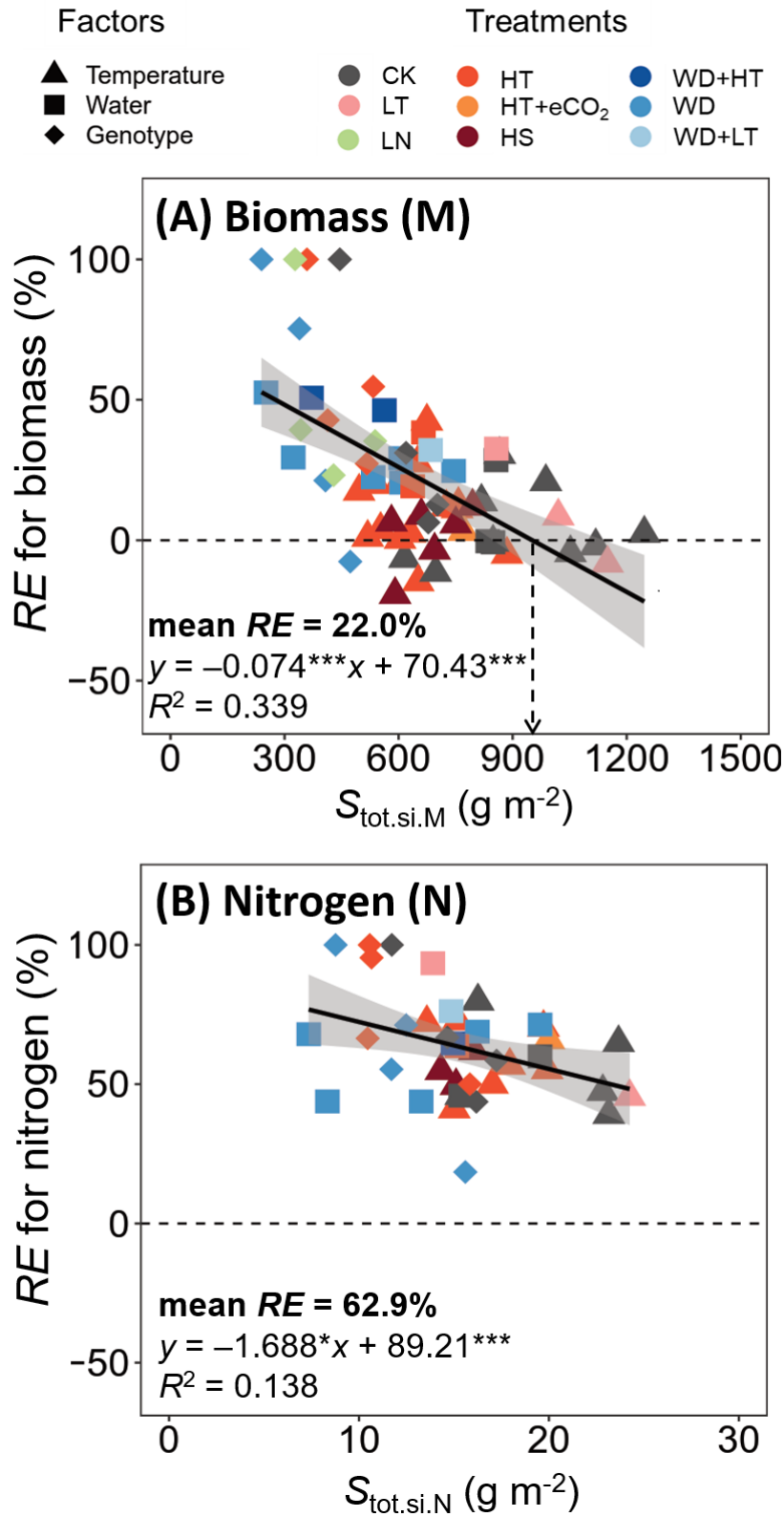
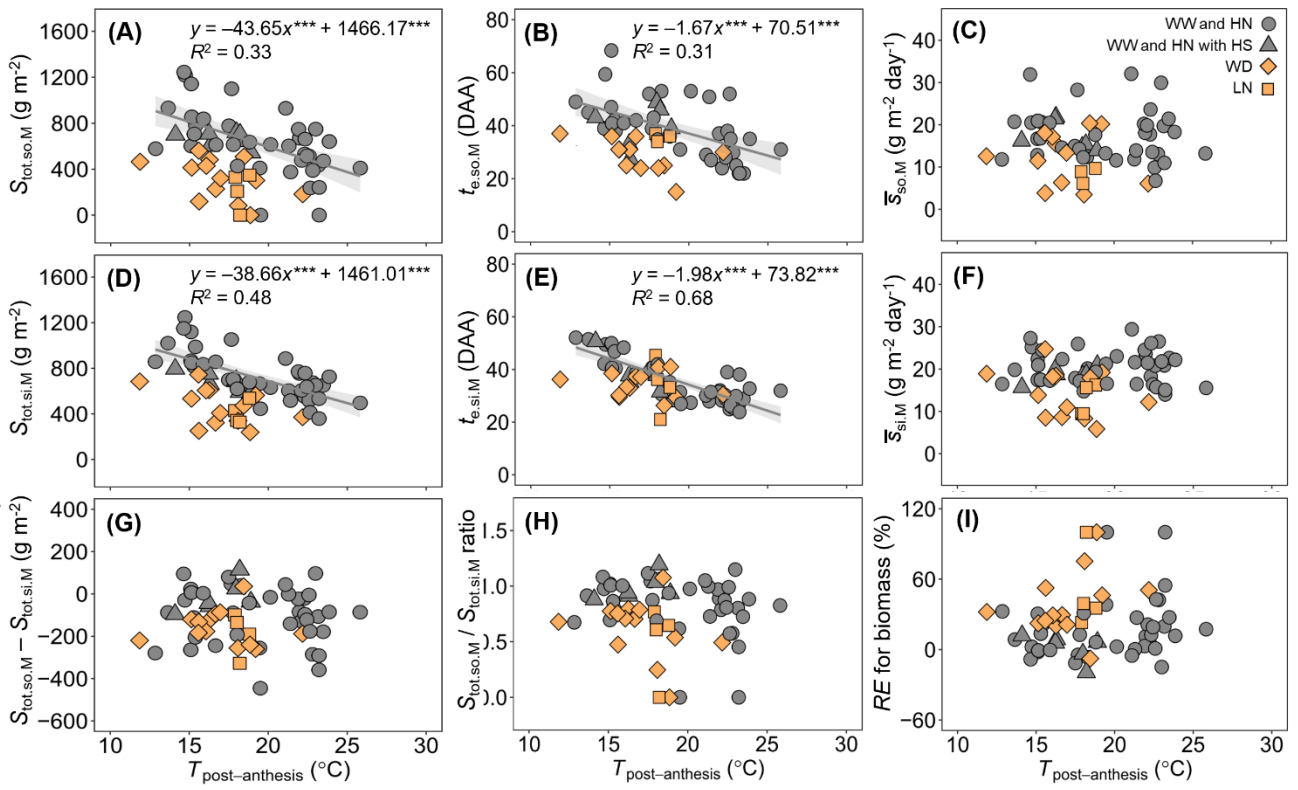
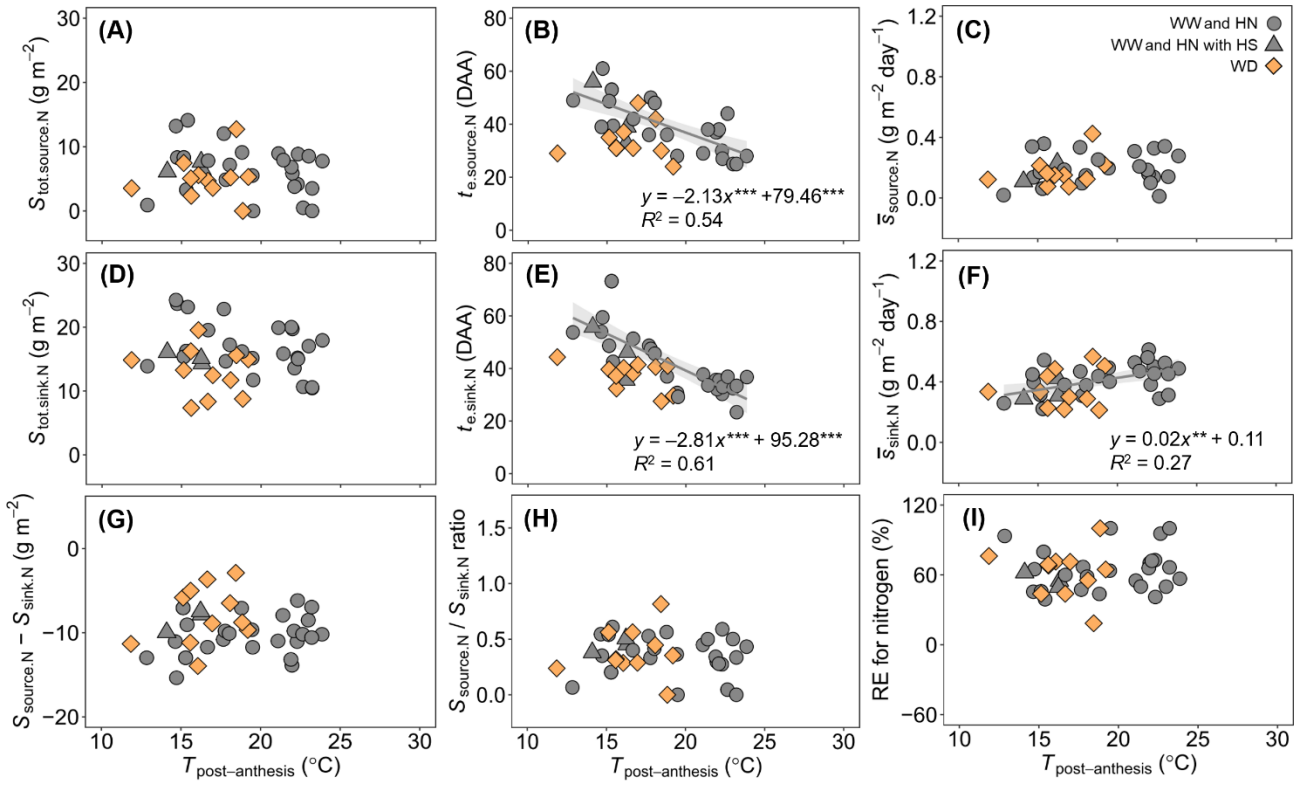


Figure 5



Accepted Manuscript

Figure 6



Accepted Manuscript